

REPORT DOCUMENTATION PAGE

READ INSTRUCTIONS
FOR USE OF TABLES FORM

AD A100153

1. REPORT NUMBER
2. AUTHOR
3. TITLE
4. SYNOPSIS
5. ABSTRACT

6. PERIODICITY
7. DISTRIBUTION STATEMENT (of this Report)
8. DISTRIBUTION STATEMENT (of the abstract entered in Block 20 if different from Report)

9. SUPPLEMENTARY NOTES
10. KEY WORDS (continue on reverse side if necessary and identify by block number)

11. ABSTRACT (continue on reverse side if necessary and identify by block number)

12. REPORT DATE
13. NUMBER OF PAGES
14. SECURITY CLASS. OF THIS REPORT
15. DECLASSIFICATION/CONTROLLING AUTHORITY
16. DISTRIBUTION STATEMENT (of this Report)

17. DISTRIBUTION STATEMENT (of the abstract entered in Block 20 if different from Report)

18. SUPPLEMENTARY NOTES
19. KEY WORDS (continue on reverse side if necessary and identify by block number)

20. ABSTRACT (continue on reverse side if necessary and identify by block number)

21. DISTRIBUTION STATEMENT (of this Report)

22. DISTRIBUTION STATEMENT (of the abstract entered in Block 20 if different from Report)

23. DISTRIBUTION STATEMENT (of this Report)

24. DISTRIBUTION STATEMENT (of the abstract entered in Block 20 if different from Report)

25. DISTRIBUTION STATEMENT (of this Report)

26. DISTRIBUTION STATEMENT (of the abstract entered in Block 20 if different from Report)

27. DISTRIBUTION STATEMENT (of this Report)

28. DISTRIBUTION STATEMENT (of the abstract entered in Block 20 if different from Report)

29. DISTRIBUTION STATEMENT (of this Report)

30. DISTRIBUTION STATEMENT (of the abstract entered in Block 20 if different from Report)

31. DISTRIBUTION STATEMENT (of this Report)

32. DISTRIBUTION STATEMENT (of the abstract entered in Block 20 if different from Report)

33. DISTRIBUTION STATEMENT (of this Report)

34. DISTRIBUTION STATEMENT (of the abstract entered in Block 20 if different from Report)

35. DISTRIBUTION STATEMENT (of this Report)

36. DISTRIBUTION STATEMENT (of the abstract entered in Block 20 if different from Report)

37. DISTRIBUTION STATEMENT (of this Report)

38. DISTRIBUTION STATEMENT (of the abstract entered in Block 20 if different from Report)

39. DISTRIBUTION STATEMENT (of this Report)

40. DISTRIBUTION STATEMENT (of the abstract entered in Block 20 if different from Report)

41. DISTRIBUTION STATEMENT (of this Report)

42. DISTRIBUTION STATEMENT (of the abstract entered in Block 20 if different from Report)

43. DISTRIBUTION STATEMENT (of this Report)

44. DISTRIBUTION STATEMENT (of the abstract entered in Block 20 if different from Report)

45. DISTRIBUTION STATEMENT (of this Report)

46. DISTRIBUTION STATEMENT (of the abstract entered in Block 20 if different from Report)

47. DISTRIBUTION STATEMENT (of this Report)

48. DISTRIBUTION STATEMENT (of the abstract entered in Block 20 if different from Report)

49. DISTRIBUTION STATEMENT (of this Report)

50. DISTRIBUTION STATEMENT (of the abstract entered in Block 20 if different from Report)

51. DISTRIBUTION STATEMENT (of this Report)

52. DISTRIBUTION STATEMENT (of the abstract entered in Block 20 if different from Report)

53. DISTRIBUTION STATEMENT (of this Report)

54. DISTRIBUTION STATEMENT (of the abstract entered in Block 20 if different from Report)

55. DISTRIBUTION STATEMENT (of this Report)

56. DISTRIBUTION STATEMENT (of the abstract entered in Block 20 if different from Report)

57. DISTRIBUTION STATEMENT (of this Report)

58. DISTRIBUTION STATEMENT (of the abstract entered in Block 20 if different from Report)

59. DISTRIBUTION STATEMENT (of this Report)

60. DISTRIBUTION STATEMENT (of the abstract entered in Block 20 if different from Report)

61. DISTRIBUTION STATEMENT (of this Report)

62. DISTRIBUTION STATEMENT (of the abstract entered in Block 20 if different from Report)

63. DISTRIBUTION STATEMENT (of this Report)

64. DISTRIBUTION STATEMENT (of the abstract entered in Block 20 if different from Report)

65. DISTRIBUTION STATEMENT (of this Report)

66. DISTRIBUTION STATEMENT (of the abstract entered in Block 20 if different from Report)

67. DISTRIBUTION STATEMENT (of this Report)

68. DISTRIBUTION STATEMENT (of the abstract entered in Block 20 if different from Report)

69. DISTRIBUTION STATEMENT (of this Report)

70. DISTRIBUTION STATEMENT (of the abstract entered in Block 20 if different from Report)

71. DISTRIBUTION STATEMENT (of this Report)

72. DISTRIBUTION STATEMENT (of the abstract entered in Block 20 if different from Report)

73. DISTRIBUTION STATEMENT (of this Report)

74. DISTRIBUTION STATEMENT (of the abstract entered in Block 20 if different from Report)

75. DISTRIBUTION STATEMENT (of this Report)

76. DISTRIBUTION STATEMENT (of the abstract entered in Block 20 if different from Report)

77. DISTRIBUTION STATEMENT (of this Report)

78. DISTRIBUTION STATEMENT (of the abstract entered in Block 20 if different from Report)

79. DISTRIBUTION STATEMENT (of this Report)

80. DISTRIBUTION STATEMENT (of the abstract entered in Block 20 if different from Report)

81. DISTRIBUTION STATEMENT (of this Report)

82. DISTRIBUTION STATEMENT (of the abstract entered in Block 20 if different from Report)

83. DISTRIBUTION STATEMENT (of this Report)

84. DISTRIBUTION STATEMENT (of the abstract entered in Block 20 if different from Report)

85. DISTRIBUTION STATEMENT (of this Report)

86. DISTRIBUTION STATEMENT (of the abstract entered in Block 20 if different from Report)

87. DISTRIBUTION STATEMENT (of this Report)

88. DISTRIBUTION STATEMENT (of the abstract entered in Block 20 if different from Report)

89. DISTRIBUTION STATEMENT (of this Report)

90. DISTRIBUTION STATEMENT (of the abstract entered in Block 20 if different from Report)

91. DISTRIBUTION STATEMENT (of this Report)

92. DISTRIBUTION STATEMENT (of the abstract entered in Block 20 if different from Report)

93. DISTRIBUTION STATEMENT (of this Report)

94. DISTRIBUTION STATEMENT (of the abstract entered in Block 20 if different from Report)

95. DISTRIBUTION STATEMENT (of this Report)

96. DISTRIBUTION STATEMENT (of the abstract entered in Block 20 if different from Report)

97. DISTRIBUTION STATEMENT (of this Report)

98. DISTRIBUTION STATEMENT (of the abstract entered in Block 20 if different from Report)

99. DISTRIBUTION STATEMENT (of this Report)

100. DISTRIBUTION STATEMENT (of the abstract entered in Block 20 if different from Report)

2
①

LEVEL

DTIC
OCT 26 1981
H

29 SEP 1981

FREDRIC C LYNCH Major, USA
Director of Public Affairs
Air Force Institute of Technology (AIC)
Wright Patterson AFB, OH 45433

DTIC FILE COPY

AFIT RESEARCH ASSESSMENT

The purpose of this report is to evaluate the value and potential of research currently being conducted in the area of the subject of the research project. The following details are requested:

AFIT No. _____
AFIT Research Project No. _____

RESEARCH TITLE: **Synoptic Climatology of Bell-Shaped Thunderstorms**

AUTHOR: **Capt Carlton R. Parks**

RESEARCH ASSESSMENT QUESTION

1. Do you believe that the research project is of sufficient value to merit AFIT support?

Yes No

2. Do you believe that the research project is of sufficient value to merit AFIT support? If not, please explain the reasons for your answer.

Yes No

3. The benefits of AFIT research are often expressed in terms of the value of the research project to the Air Force. What is the value of the research project to the Air Force? Please explain the value of the research project in terms of manpower and/or dollars.

Yes No

4. Often the value of the research project is expressed in terms of the results of the research project. Do you believe that the research project is of equivalent value to the research project? What is your estimate of the value of the research project?

Yes No

5. AFIT welcomes any further comments you may have on the above questions. Any additional details concerning the present application, future potential, or other value of the research project. Please use the bottom part of this questionnaire for your statements.

NAME: _____ GRADE: _____ POSITION: _____

ORGANIZATION: _____ LOCATION: _____

STATEMENT(S):

A

FOLD DOWN ON OUTSIDE - SEAL WITH TAPE

AFIT/ NR
WRIGHT-PATTERSON AFB OH 45433
OFFICIAL BUSINESS
PENALTY FOR PRIVATE USE \$300



NO POSTAGE
NECESSARY
IF MAILED
IN THE
UNITED STATES

BUSINESS REPLY MAIL
FIRST CLASS PERMIT NO 7326 WASHINGTON D C

POSTAGE WILL BE PAID BY ADDRESSEE

AFIT/ DAA
Wright-Patterson AFB OH 45433



FOLD IN

81-27T

THE UNIVERSITY OF OKLAHOMA
GRADUATE COLLEGE

(6) SYNOPTIC CLIMATOLOGY OF
BELL-SHAPED THUNDERSTORMS.

14) A FIT-182-27T

(9) ... thesis

A THESIS
SUBMITTED TO THE GRADUATE FACULTY
in partial fulfillment of the requirements for the
degree of

MASTER OF SCIENCE
IN METEOROLOGY
84 pp

(12) 96

(10) By
CAPTAIN, USAF
CARLTON B. PARKS
Norman, Oklahoma

11) 1981

81 - 0 6 209

012200

Abstract

Eleven cases of bell-shaped thunderstorm occurrence are analyzed for characteristic features of synoptic patterns, vertical wind shear, and temperature and moisture stratification. Comparisons are made with certain well-documented supercell and multi-cell cases. A model synoptic pattern, sounding, and hodograph are presented.

Major findings are: (1) The storms formed in a highly unstable environment just ahead of a dryline, often near a dryline/front intersection. (2) A strong upper-level disturbance was not required to trigger the storms. (3) The storms formed as isolated cells, often to the south of a broken line of existing storms, and often continued as isolated cells for several hours. (4) Except for being slightly more unstable, the environment of the storms did not differ significantly from that of the supercells, but did differ significantly from that of the multi-cell storms. (5) An intense updraft, and the absence of a water-loaded downdraft, may be responsible for many of the physical characteristics of the storms.

SYNOPTIC CLIMATOLOGY OF
BELL-SHAPED THUNDERSTORMS

A THESIS

APPROVED FOR THE DEPARTMENT OF METEOROLOGY

By

Howard B. Bluestein

Robert P. Janis-Jones

Don W. Burgess

John H. Johnson

ACKNOWLEDGEMENTS

I am deeply grateful to Dr. Howard Bluestein and Dr. Rex Inman for their guidance and encouragement during the preparation of this manuscript, and to Dr. Robert Davies-Jones for his suggestions and helpful criticism. Sincere appreciation is extended to Mr. Don Burgess who provided needed data from the National Severe Storms Laboratory, and who gave generously of his time and ideas.

Mr. Eric Rasmussen of Texas Tech, Mr. Gene Moore of Channel 43 television in Oklahoma City, and Mr. David Hoadley of Falls Church, Virginia provided storm descriptions that were essential to this work. Dr. Barney Meisner suggested statistical tests which were most useful. I also wish to thank Terry Snodgrass and Christi Hull for their superb typing and patience through many revisions.

This study was made possible through my assignment to the Air Force Institute of Technology, Wright-Patterson AFB, Ohio. Partial support was provided through National Science Foundation Grant ATM-7923649.

Abstract

Eleven cases of bell-shaped thunderstorm occurrence are analyzed for characteristic features of synoptic patterns, vertical wind shear, and temperature and moisture stratification. Comparisons are made with certain well-documented supercell and multi-cell cases. A model synoptic pattern, sounding, and hodograph are presented.

Major findings are: (1) The storms formed in a highly unstable environment just ahead of a dryline, often near a dryline/front intersection. (2) A strong upper-level disturbance was not required to trigger the storms. (3) The storms formed as isolated cells, often to the south of a broken line of existing storms, and often continued as isolated cells for several hours. (4) Except for being slightly more unstable, the environment of the storms did not differ significantly from that of the supercells, but did differ significantly from that of the multi-cell storms. (5) An intense updraft, and the absence of a water-loaded downdraft, may be responsible for many of the physical characteristics of the storms.

TABLE OF CONTENTS

	Page
Acknowledgments.....	iii
Abstract.....	iv
List of Figures.....	vii
List of Tables.....	ix
Chapter	
I. INTRODUCTION.....	1
II. METHODOLOGY.....	5
III. CASE STUDIES.....	8
Case 1, 26 May 1963.....	8
Case 2, 4 June 1973.....	9
Case 3, 5 June 1974.....	11
Case 4, 5 December 1975.....	12
Case 5, 26 April 1976.....	13
Case 6, 27 April 1976.....	15
Case 7, 30 April 1978.....	17
Case 8, 16 May 1978.....	18
Case 9, 24 May 1978.....	19
Case 10, 30 May 1978.....	20
Case 11, 20 June 1979.....	21
IV. SUMMARY AND CONCLUSIONS.....	24

	Page
V. RECOMMENDATIONS FOR FURTHER STUDY.....	31
Bibliography.....	33
Appendix.....	36

LIST OF FIGURES

Figure	Page
1. Sketch of the bell-shaped storm of 4 June 1973..	38
2. Sketch of the bell-shaped storm of 26 May 1963..	39
3. Photograph of the bell-shaped storm of 16 May 1978.....	40
4. Surface analysis 1500 CST, 26 May 1963.....	41
5. Radar depiction of storm formation, 26 May 1963.....	42
6. Surface analysis 1600 CST, 4 June 1973.....	43
7. Radar depiction, 4 June 1973.....	44
8. Surface analysis 1800 CST, 5 June 1974.....	45
9. Radar depiction, 5 June 1974.....	46
10. Surface analysis 1500 CST, 5 December 1975.....	47
11. Radar depiction, 5 December 1975.....	48
12. Surface analysis 1500 CST, 26 April 1976.....	49
13. Radar depiction, 26 April 1976.....	50
14. Surface analysis 1500 CST, 27 April 1976.....	51
15. Radar depiction, 27 April 1976.....	52
16. Surface analysis 1500 CST, 30 April 1978.....	53
17. Radar depiction, 30 April 1978.....	54
18. Surface analysis 1800 CST, 16 May 1978.....	55
19. Radar depiction, 16 May 1978.....	56

Figure	Page
20. Surface analysis 1800 CST, 24 May 1978.....	57
21. Radar depiction, 24 May 1978.....	58
22. Surface analysis 1500 CST, 30 May 1978.....	59
23. Radar depiction, 30 May 1978.....	60
24. Surface analysis 1500 CST, 20 June 1979.....	61
25. Radar depiction, 20 June 1979.....	62
26. Hodograph, 26 May 1963.....	63
27. Hodograph, 4 June 1973.....	64
28. Hodograph, 5 June 1974.....	65
29. Hodograph, 5 December 1975.....	66
30. Hodograph, 26 April 1976.....	67
31. Hodograph, 27 April 1976.....	68
32. Hodograph, 30 April 1978.....	69
33. Hodograph, 16 May 1978.....	70
34. Hodograph, 24 May 1978.....	71
35. Hodograph, 30 May 1978.....	72
36. Hodograph, 20 June 1979.....	73
37. Water content in relation to updraft speeds...	74
38. Model morning sounding for days of bell-shaped storm occurrence.....	75
39. Model sounding near time of bell-shaped storm development.....	76
40. Model hodograph of environmental winds near bell-shaped storms.....	77
41. Model surface features near time of bell-shaped storm development.....	78

LIST OF TABLES

Table		Page
1.	Thermodynamic parameters of the environment in which bell-shaped storms occur.....	79
2.	Stability and wind shear parameters of the environment in which bell-shaped storms form...	80
3.	Stability and wind shear parameters for certain well-documented supercell storms.....	81
4.	Stability and wind shear parameters for certain well-documented multi-cell storms.....	82
5.	Hodograph turning with height for bell-shaped storms.....	83
6.	Hodograph turning with height for certain well-documented supercell storms.....	83
7.	Key parameters in forecasting severe storms....	84

SYNOPTIC CLIMATOLOGY OF BELL-SHAPED THUNDERSTORMS

CHAPTER I

INTRODUCTION

A few cases of bell-shaped thunderstorms which formed along a dryline and produced tornadoes and large hail have been documented. Because of the unique appearance of the cloud in these dryline storm cases, the term bell-shaped storm will be used in this study. Davies-Jones *et al.* (1976) described a cyclonically rotating bell-shaped thunderstorm (Fig. 1) which passed over the National Severe Storms Laboratory (NSSL) and produced a tornado and baseball size hail, but only light rainfall. The storm appeared relatively weak on the WSR-57 radar at NSSL, satisfying none of the National Weather Service guidelines for severe weather warnings. However, at mid-levels the radar echo did have an overhang capping the updraft. Outstanding visual features of the storm were the bell-shaped cloud with a flared-out base, an almost vertical south wall with helical striations, and pronounced mamma hanging from an extensive anvil. A ring of mid-level cloud circled the storm. A wall cloud (Fujita 1959) hanging from the base of the bell-shaped cloud contained a

hollow doughnut-like structure showing more rapid rotation than the rest of the cloud. It was suggested that the storm consisted of a large rotating updraft so intense that most precipitation particles were carried downstream in the anvil rather than falling back through or out of the updraft as discussed by Kessler, 1969, p. 74.

Burgess and Davies-Jones (1979) documented storms strikingly similar to the one just described. These storms also appeared weak on radar and were never intense enough to justify a severe storm warning based on radar alone. Storm size and weak low-level echo without hook were not consistent with Browning's (1957) supercell model; however, tornadoes and baseball size hail occurred. Burgess and Davies-Jones surmised that an intense updraft at the rear flank of the storm carried precipitation particles far aloft before they reached radar detectable sizes and allowed only hail and a few large raindrops to reach the ground before evaporating.

Browning (1965) draws on the accounts of several trained observers to present a unified description of a bell-shaped storm (Fig. 2) near Oklahoma City. From close to the level of its flared base, near 4,000 feet, the cloud wall was nearly vertical to near 30,000 feet where it penetrated the dense anvil of another storm. A sharply defined ring of light surrounded the bell cloud where it penetrated

the anvil. Between the center and the southwestern edge of the bell cloud base, a cyclonically rotating vortex rim composed of a smooth roll cloud was observed. There appeared to be a hole within this rim from which a soft white light of blue-green hue was shed. A funnel cloud formed near this position a short time later and developed into a tornado. Hail up to $3\frac{1}{4}$ inches in diameter was observed outside the wall of the bell cloud but no precipitation was visible beneath it except at the northern edge.

A cyclonically rotating bell-shaped thunderstorm (Fig. 3) in Texas has also been documented (Bluestein et al., 1978). Time-lapse movies of much of the life history of this storm were taken by a storm-intercept team from the University of Oklahoma. The movies indicated inflow at most levels of the storm and no large area of precipitation beneath cloud base. The conclusion was that the storm's outflow was through the anvil only, except during the storm's collapse. A high-based funnel cloud was seen to the north of the cloud base wall. Storm dissipation was marked by the base increasing in width while the mid-section decreased to a narrow tube then collapsed. The thick anvil produced a spectacular display of mamma after the storm collapsed. It was hypothesized that the storm updraft may have been inhibited by strong rotation as in a vortex valve (Lemon, 1976).

These cases, and others which have not been published, describe storms quite different from the classic hail or tornado producing supercell as was pointed out by Burgess and Davies-Jones (1979). Because of the deceptively weak appearance of these bell-shaped storms on radar, adequate warning of the severe weather they produce may not be possible from what is now known.

The purpose of this thesis is to determine any characteristic features of synoptic patterns, vertical wind shear, or temperature and moisture stratification associated with this type of storm. Any such identifiable features would not only assist in forecasting storms of this nature, but possibly could be of value in numerical modeling and lead to a more complete understanding of storm dynamics.

CHAPTER II

METHODOLOGY

The overall methodology has been to first describe the storms and the environment in which they form, and then to compare these cases with well-documented supercell and multi-cell storm cases. Marwitz (1972a, 1972b) used a similar approach.

Surface charts have been plotted, starting at 0600 Central Standard Time (CST), for each of the eleven storm cases. Wind direction was plotted to the nearest 10 deg with the tens digit indicated at the end of the shaft. Wind speed was plotted in kts. Since all stations do not report sea level pressure every hour, altimeter settings were used for pressure to increase data density. A plot of 995 represents 29.95 inches of mercury. Temperature and dew point were plotted in deg Fahrenheit.

Standard and special release upper air soundings were plotted for stations representative of the location where storm formation took place. Wind hodographs were constructed from these soundings to identify changes in wind shear with height more easily.

Surface charts were analyzed to locate pressure centers, fronts, and other synoptic features. Upper air soundings have been analyzed for temperature and moisture stratification, and air mass stability. A lifted index (Galway, 1956) for each sounding was determined using the average mixing ratio in the moist layer and the observed maximum surface temperature near the location of storm formation.

Klemp and Wilhelmson (1978a, 1978b) have shown that the profile of vertical wind shear is important in the behavior of simulated convective storms. Their three-dimensional model was first initialized using a convectively unstable sounding and a vertical wind profile in which the hodograph was unidirectional with height. During the simulation the initial updraft split into two parts which moved laterally apart with the right-moving updraft rotating cyclonically, the left-moving one anticyclonically. Next, the wind profile was changed so that the hodograph turned clockwise with height. Storm splitting again occurred, but the left-moving storm was weaker than the right-moving storm and decayed with time. Finally, a wind profile in which the hodograph turned counterclockwise with height was used. Splitting again occurred, but this time the right-moving storm was weaker.

In order to produce the most representative verti-

cal wind profile, composite hodographs have been constructed using linear interpolation to combine morning and evening hodographs. Surface wind for the hodograph was taken from a report near the time and location the storm began. For each case, the amount of turning (θ) with height (H) was determined from the surface up to the point where the hodograph became unidirectional or reversed its direction of turning. The ratio $\frac{\theta}{H}$ was calculated as a means of comparing hodographs of bell-shaped storm cases with those of supercell or multi-cell storm cases.

Radar film has been analyzed to determine if there is a preferred location for bell-shaped thunderstorms to form in relation to other storms. Eyewitness accounts of storm location have assisted in determining which radar echoes represented bell-shaped storms.

In addition to the locally prepared charts already mentioned, charts prepared by the National Meteorological Center were used to help describe the synoptic situation.

The reader may wish to refer to the appendix for a brief summary of synoptic features favorable for severe thunderstorm development.

CHAPTER III

CASE STUDIES

Case 1, 26 May 1963

At 0600 CST synoptic conditions were as follows:

At the surface there was a weak low pressure center in the Texas Panhandle with a cold front extending into New Mexico and a warm front across southern Oklahoma. There was a dryline between Amarillo and Childress, Texas extending to the southwest. Dew points were in the mid to upper 60's over southern Oklahoma. At 500 mb there was a closed low in South Dakota with a trough extending southward into eastern New Mexico. A high level jet over New Mexico split with one branch across northwest Oklahoma and the other over central Texas. A region of diffluence was apparent over central Oklahoma. The Oklahoma City sounding indicated a lifted index of -10 for a high temperature of 91°F.

By 1500 CST the surface low had deepened and moved to just west of Oklahoma City (Fig. 4). A line of thunderstorms had developed east of the low and the first echo of what was to become the bell-shaped storm described by Browning (1965) had just formed along the dryline (Fig. 5).

Browning explained the appearance of the dryline on radar as probably due to a sharp discontinuity of refractive index across the dryline. The dryline/front intersection was only a few miles northwest of where the bell shaped storm first appeared. This intersection is known to be a preferred region for thunderstorm development (Tegtmeier, 1974).

A special sounding was released at 1420 CST from Oklahoma City just ahead of the storm. The lifted index was -8.4 and there was deep layer in which the lapse rate was near dry adiabatic. Winds veered strongly in the low levels and the hodograph showed a $\frac{\theta}{H}$ of 40 deg km⁻¹.

Case 2, 4 June 1973

The synoptic setting for this case is similar to that of the first. At 0600 CST a weak surface low was centered near Gage, Oklahoma; a front extended westward south of Dalhart, Texas and northeastward across central Kansas. A dryline extended to the southwest between Childress and Lubbock, Texas. Dew points were in the 60's east of the dryline and in the 40's to the west. At 350 mb a moist tongue was evident over central Oklahoma ahead of a warm thermal ridge. A closed low at 500 mb was north of North Dakota with a trough extending southward east of the Rocky Mountains. Cold air advection at 500 mb over Oklahoma was weak by appeared to lead that at 700 mb. Upper level winds were under 25 m s⁻¹, which is relatively weak.

The 0600 sounding at Tinker Air Force Base (TIK) showed a moist layer 850 m deep capped by an inversion. There was greater than dry adiabatic lapse rate indicated between 600 and 700 mb. The lifted index for a maximum temperature of 92°F was -7.3. Winds veered with height to above 1 km.

By 1600 CST dew points in central Oklahoma had increased to the 70's and the synoptic pattern was as shown in Fig. 6. Thunderstorms were forming along the front and dryline northwest of Oklahoma City. At 1615 CST the first echo of the bell-shaped storm described by Davies-Jones et al., (1976) appeared on the National Severe Storms Laboratory (NSSL) radar. Fig. 7 shows the storm forming south of a broken line of thunderstorms along the dryline. The storm intensified and moved to the east-northeast at 20 kts but remained weaker on radar than storms to the north. Almost three hours after it appeared on radar, this storm produced baseball size hail and a brief tornado.

As in Case 1, this bell-shaped storm formed along a dryline not far from the dryline/front intersection. Since there were no special soundings near the time the storm formed, a composite hodograph was constructed from the 0600 and 1800 CST soundings from TIK. In this case, $\frac{\theta}{H}$ equals 27.8 deg km⁻¹.

Case 3, 5 June 1974

On 5 June 1974 a storm (which was not described in the introduction) occurred near Hays, Kansas. Although details on this storm are sketchy, a photograph taken by David Hoadley of Falls Church, Virginia is quite graphic. It shows a circularly symmetric cloud base, concave in the center. The laminar sides of the cloud had striations suggesting rotation. Mr. Hoadley's notes confirm that the cloud was rotating counterclockwise very rapidly. The storm produced a brief funnel and hail falling at a 45 deg angle to the horizon.

At 0700 CST the surface chart showed a fast moving cold front across southwest Nebraska and southeastern Colorado. A poorly defined dryline extended south of the front from Colorado to eastern New Mexico. A low pressure trough was well to the east of this dryline in central Kansas and Oklahoma. Dew points in central Kansas were in the mid 50's. A closed low at 500 mb was north of Montana with a trough extending southward to northern Utah. A strong jet at 300 mb was moving south-eastward into northwest Utah. Upper level flow was diffluent over Kansas.

The 0600 CST sounding at Dodge City showed a fairly deep moist layer capped by an inversion and a near dry adiabatic lapse rate above. For a maximum temperature of 93°F, the lifted index was -8.4. The hodograph showed light

and variable winds at all levels.

Throughout the day the cold front advanced southward and the dryline strengthened and moved eastward. By 1800 CST a well defined dryline/front intersection marked the center of a still deepening low north of Dodge City (Fig. 8). The storm photographed by Mr. Hoadley had formed very near this intersection just south of a squall line as seen from the Garden City, Kansas radar (Fig. 9).

The Dodge City sounding at 1800 CST was taken to be the best representation of the environment where the storm occurred.

Case 4, 5 December 1975

This case was mentioned in the introduction and has been described in detail by Burgess and Davies-Jones (1979). It is unique in that it did not occur in April, May, or June as did all other cases of this study.

At 0600 CST a weak low was in the Oklahoma Panhandle; a cold front extended from western Kansas to eastern New Mexico. Dew points in central Oklahoma were in the low 60's ahead of a dryline in the western part of the state.

In mid-levels, winds were from the southwest at about 30 m s^{-1} ahead of a trough that was to move across the state during the day. Maximum winds on the Oklahoma City sounding at 0600 CST were 35 m s^{-1} at 7 km. This sounding also showed the moist layer to be deep, greater

than 2 km. The lifted index was -5.7 for a maximum temperature of 69°F.

During the day the surface low moved eastward and began to fill. By 1500 CST the low was west of Ponca City and the dryline curved south-eastward past Enid, Oklahoma City, and Ardmore (Fig. 10). The moisture gradient across the dryline is obvious from Tulsa's dew point of 61°F and Oklahoma City's 34°F. Radar at this time showed a line of echoes forming just ahead of the dryline (Fig. 11). Within two hours, baseball-size hail and 4 tornadoes had occurred from echoes along this line.

Burgess and Davies-Jones noted the likeness of these storms and the 4 June 1973 case. In addition to both cases occurring ahead of drylines, most precipitation reached the ground as hail or a few large raindrops, possibly because of intense updrafts. Both cases produced tornadoes and large hail while having rather weak radar appearances. Also in both cases storm cells had long isolated lifetimes.

Case 5, 26 April 1976

On the morning of 26 April 1976 a surface low was in southern Colorado ; a cold front dipped southward into New Mexico and a warm front was forming eastward along the Kansas-Oklahoma border. A dryline could be identified in eastern New Mexico. In the Texas Panhandle where the bell-

shaped storm formed later, dew points were only in the low 40's.

At upper levels, a deep closed low at 500 mb was centered in northwest Utah; however, vorticity advection into Texas appeared weak. Warm, moist air was being advected into northwest Texas at 850 mb. Weak diffluence could be seen at 300 mb but the jet at that level appeared to be too far to the northwest to trigger severe weather in Texas.

The 0600 CST Amarillo sounding showed a moist layer 390 m deep capped by a strong inversion. A lifted index of -5 was indicated if a maximum temperature of 80°F was reached. Low level winds veered sharply up to 4 km.

By 1500 CST a bulge in the dryline (portion of the dryline which has advanced most rapidly) had developed east of Clovis, New Mexico (Fig. 12). Within a few minutes, three small cells could be seen on radar about 40 miles southwest of Amarillo (Fig. 13) just ahead of the bulging dryline. Amarillo was reporting only 60°F but temperatures to the south were much warmer. Lubbock was reporting 84°F. The cells moved southeast of Amarillo, intensified very rapidly, and became almost stationary. Gene Moore of NSSL and now with Channel 43 television in Oklahoma City was on hand to observe the bell-shaped thunderstorm near Silverton, Texas. In personal communication with the author, he described the storm as quite symmetric with a slightly flared

base and a vertical mid-section having striations that gave the impression of "a hugh twisted towel". The cloud base was almost completely free of precipitation and contained a cloud-free hole near the center. There was a backsheared anvil with mamma. Large hail was seen falling from the sides of the storm and a brief high-based funnel was observed to cause dust whirls on the ground. Mr. Moore remarked that the storm seemed to have become anchored over the caprock (an abrupt rise in terrain) southeast of Amarillo and was definitely feeding on warm moist flow from the south.

A composite hodograph of the morning and evening soundings from Amarillo shows 115 deg of turning in 3.7 km for a $\frac{\theta}{H}$ of 31.1 deg km⁻¹.

Case 6, 27 April 1976

This case occurred only one day after Case 5 and the morning synoptic situation was much the same. The surface low was now in northeastern New Mexico. Fronts were almost stationary across central New Mexico and along the Kansas-Oklahoma border. A dryline extended from the low southward to the west of Roswell and Carlsbad, New Mexico. Dew points were now in the mid 50's in the Texas Panhandle where the bell-shaped storm was later to form.

Warm, moist air continued to be advected at 850 mb. The low at 500 mb was still centered in northwest Utah and

vorticity advection remained weak. The jet at 300 mb had moved closer to the Texas Panhandle but was not in an ideal location for severe weather.

The Amarillo morning sounding showed that the moist layer had thickened to more than 1 km. A steep lapse rate above an inversion was apparent. For a maximum temperature of 80°F, the lifted index was computed to be -8.5. Low-level winds veered up to 4.7 km. The deeper moist layer and high instability pointed more to severe weather on this day than on the previous one.

During the day, the surface low moved eastward and by 1500 CST the dryline/front intersection was just northwest of Dalhart, Texas (Fig. 14). Amarillo radar at 1450 CST (Fig. 15) depicted a broken line of echoes developing ahead of the dryline. A cell forming southeast of Dalhart was later observed to be a bell-shaped storm. Steve Tegtmeier, formerly at the University of Oklahoma, who observed this storm, could not be contacted by the author for a first hand account of what he had seen. However, he had described the storm to Mr. Gene Moore who confirmed the cloud was almost identical, except for a smaller size and an appreciable tilt, to the storm he had seen the previous day. This storm also produced a high-based funnel which caused dust whirls on the ground.

Case 7, 30 April 1978

On the morning of 30 April 1978, a surface low was located in the Texas Panhandle southwest of Gage, Oklahoma. A cold front from the low entered New Mexico and a warm front to the east crossed Oklahoma south of Tulsa. A dry-line extended southward west of Abilene. Fog covered much of Oklahoma and dew points were in the 60's.

A low at 850 mb was centered west of Amarillo and became an open wave at 700 mb. The axis of the 700 mb thermal ridge lay northwest to southeast just east of Amarillo. Positive vorticity advection at 500 mb was soon to begin over Oklahoma.

The 0600 CST Oklahoma City sounding showed the depth of the moist layer to be 1200 m. An absolutely stable lapse rate to near 750 mb changed to near dry adiabatic to above 500 mb.

The surface low moved to the southeast and by 1500 CST was centered near Hobart, Oklahoma (Fig. 16). An echo on the NSSL radar was seen growing east of Fort Sill at this time (Fig. 17). The cell intensified and moved to the northeast where it was observed by University of Oklahoma and NSSL storm-chase teams. Between 1700 and 1800 CST it produced 3/4 inch hail and a funnel near Rush Springs. The cloud was seen to have a flared base and to be rotating.

Case 8, 16 May 1978

The bell-shaped storm in this case formed northwest of Breckenridge, Texas on 16 May 1978. It was discussed in the introduction and has been described more fully by Bluestein et al. (1978).

The main features on the 0600 CST surface chart were a low in north central Texas, an east-west oriented front, and a dryline extending to the southwest. Dew points ahead of the dryline were in the upper 60's and lower 70's. Just behind the dryline, Abilene reported a dew point of 55°F while further to the west dew points were near 20°F. Above the surface, winds were light and variable.

The morning sounding from Stephenville showed a surface-based moist layer 520 m deep and another moist layer around 500 mb. The lapse rate was steep between these layers. The lifted index was found to be -8.9 for a high temperature of 91°F.

By 1800 CST surface conditions were as shown in Fig. 18. Abilene was reporting a temperature of 102°F with a dew point of 22°F. Ahead of the dryline, temperatures were in the 80's with dew points in the 70's. The bell-shaped storm documented by Bluestein's group was in progress near the dryline/front intersection.

Stephenville radar at 1500 CST (Fig. 19) shows storms along the dryline and the warm front. Radar film was

not available after this time.

Case 9, 24 May 1978

This case is unique in that there is a dryline but no surface front in the vicinity of the bell-shaped storm. The 0600 CST surface chart showed a dryline weaving from eastern Colorado to southwest Texas. Dew points were in the low 60's east of the dryline and in the 30's to the west.

Above the surface, a closed low at 850 mb in Montana sloped westward to a closed 300 mb center on the Washington-Oregon border. Weak warm air advection was indicated at 850 mb and weak cold air advection at 700 mb. A southwest wind maximum of 25 m s^{-1} at 500 mb was over New Mexico. Positive vorticity advection seemed unlikely during the day.

The morning sounding at Amarillo showed a moist layer 540 m deep below an inversion. A lifted index of -9 was computed using a high temperature of 85°F.

By 1800 CST the dryline had moved to near Amarillo (Fig. 20) and thunderstorms had formed or were forming along its entire length. A thunderstorm with 1/4 inch hail had just passed over Amarillo and to the northeast.

Fig. 21 shows an echo east of Amarillo which a University of Oklahoma storm-chase team (Bluestein et al., 1978) observed to have bell-shaped storm characteristics.

A rotating tower with striations on the base and rain falling from an anvil to the northeast preceded a high-based funnel cloud. The storm grew narrower before dissipating much like Case 8. The storm-chase team reported 5/8 inch hail at the surface near this storm.

Case 10, 30 May 1978

This case, as did Case 3, occurred in Kansas. The synoptic setting of the two cases was much the same.

At 0700 CST a surface cold front was pushing into extreme northwest Kansas and northeast Colorado. A low pressure center was near the border of the two states. A dryline extended to the southwest into New Mexico; however, the moisture gradient was not strong at this time. Dew points were in the 30's west of the dryline and only in the upper 40's and low 50's to the east. Moist, warm air advection was evident in the southerly flow ahead of the low.

Strong southwest winds at 850 mb were entering southwest Kansas but temperature advection was weak. Moderate height falls were seen in Colorado ahead of the trough line extending southward from a closed 500 mb low in Montana. A 300 mb jet greater than 40 m s^{-1} was moving into northwest Colorado.

The morning sounding from Dodge City was quite dry at low levels. A strong radiation inversion from the surface to 885 mb changed to a fairly steep lapse rate to

above 500 mb. A lifted index of -6.8 was determined using 87°F for a high temperature.

By 1500 CST the surface low had deepened slightly and moved eastward (Fig. 22). Thunderstorms were forming along the dryline near Garden City (Fig. 23). The cell nearest Garden City moved to the east-southeast and was observed by Eric Rasmussen from the University of Oklahoma (now at Texas Tech). In personal communication with the author, he described the storm as having a fully circular base with a collar into which "extreme" vertical motion was observed. There was rotation visible to high levels and an extensive anvil with very large mamma. Several funnels or weak tornadoes were observed to lift dust to the base of the storm. Heavy rain and hail were falling from high levels northeast of the base. As the storm collapsed near 2000 CST, outflow winds were estimated at 35 to 40 m s^{-1} . Heavy rain and large hail accompanied the collapse of the storm.

Case 11, 20 June 1979

The bell-shaped storm in this case occurred in Oklahoma. The synoptic conditions were quite similar to the previous cases.

The surface chart at 0600 CST showed a trough of low pressure and a cold front from eastern Kansas to the Texas Panhandle. A dryline could be seen from southwest

Oklahoma to near Wink, Texas. Dew points in the upper 60's lay ahead of the dryline in central Oklahoma.

Upper level charts showed a closed low at 850 mb in southeast North Dakota with almost no vertical tilt to 300 mb. Weak warm air advection was occurring below 700 mb. Maximum winds were near 40 m s^{-1} near 200 mb over northern Oklahoma.

The morning sounding from Oklahoma City revealed a moist layer to above 1 km. An absolutely stable lapse rate from the surface to 850 mb became almost dry adiabatic to 640 mb. A surface high temperature of 94°F was used to calculate a lifted index of -5.5.

By mid-afternoon surface temperatures had climbed to the mid 90's and rainshowers were forming ahead of the dryline in Oklahoma. The 1500 CST surface chart (Fig. 24) shows a weak low pressure center and the dryline position.

Oklahoma City radar at 1513 CST (Fig. 25) shows the line orientation in which convection was taking place. Radar film was not available after this time, so exact location of where the bell-shaped storm formed is not known.

Between 1800 and 1900 CST, Dr. Howard Bluestein, (University of Oklahoma, School of Meteorology) observed and photographed a bell-shaped storm near Chickasha, Oklahoma. The cloud had a flared, circular base, concave in the center. There was a vertical mid-section with striations,

and a large anvil. A funnel was observed, and 1 inch hail fell from the anvil.

CHAPTER IV

SUMMARY AND CONCLUSIONS

Each of the eleven cases included a tornado, funnel, or hail report. A confirmed tornado was reported in four of the cases, and one or more funnels were observed in the remaining seven cases. In all cases but one, hail was observed. Reported hail size ranged from 5/8 inch to 3 1/2 inches in diameter. In four of the cases, hail was 3 inches or more in diameter.

In ten of the cases studied, the bell-shaped storm formed in the warm, moist sector near, but to the south of, a dryline/front intersection. In the remaining case, storm formation took place near a dryline, but there was no front nearby. In all cases, storm formation was within 50 km of the dryline. The average distance was 27 km. In nine of the ten cases with a dryline/front intersection, storm formation was within 200 km of the intersection (average 90 km). The distance in the remaining case was almost 400 km which raised the average distance to 120 km.

The synoptic discussion revealed that there was never any strong synoptic scale forcing to initiate severe convection. Strength and relative position of any 500 mb trough

or high-level jet was never ideal, and warm air advection at low levels was never strong. Kessinger and Bluestein (1979) have proposed that a local maximum of frontogenesis, due to deformation acting on the horizontal potential temperature gradient near the dryline/front intersection, can be related to the initiation of convection on days when upper level support is weak. A thermally-direct vertical circulation accompanies the frontogenesis and the rising portion of this circulation may act as a triggering mechanism for thunderstorm development.

The figures depicting radar echoes have been superimposed with surface features to show the location of bell-shaped storms in relation to front and dryline positions as well as to other storms. The bell-shaped storms always formed as isolated cells, often (6 of 9 cases with adequate radar data) to the south of a broken line of existing storms (some of which may have been supercells). They often continued as isolated cells for several hours. There was no evidence of any outflow boundary from storms to the north that could have influenced the development of the bell-shaped storms (Maddox et al. 1980).

Thermodynamic parameters from soundings on storm days are listed in Table 1. Parameters were computed from morning and evening soundings, then averaged with time-weight given to the sounding nearest the time of storm

formation (linear interpolation). The average thermal buoyancy at 500 mb (ΔT_{500}) from parcel theory for these cases is 7.8°C. This is considerably more than the 6°C for the tornado situations discussed by Fawbush and Miller (1954).

To place bell-shaped storms in the proper perspective, their environmental conditions have been listed in Table 2 for comparison with supercell cases (Table 3) from several authors, and multi-cell cases (Table 4) from Marwitz (1972b). The following conclusions about bell-shaped storms can be drawn from these tables:

1. They formed in a highly unstable environment (mean thermal buoyancy at 500 mb of 7.8°C compared to 6.4°C for supercells and 3.9°C for multi-cell storms).
2. The mean winds below cloud base were slightly stronger (14 m s^{-1}) and veered more (72.3°) than supercell (13.1 m s^{-1} and 62°) or multi-cell (8 m s^{-1} and 47.2°) storms.
3. Wind shear in the cloud layer was no different ($3.4 \times 10^{-3} \text{ s}^{-1}$) than for supercell ($3.4 \times 10^{-3} \text{ s}^{-1}$) storms, but was greater than that for multi-cell storms ($2.6 \times 10^{-3} \text{ s}^{-1}$).
4. Storm motion averaged 23 deg to the right of mean winds between the surface and 10 km compared to 19 deg for supercell and 36 deg for multi-cell storms.

The range of values from bell-shaped storm cases was compared to the supercell and multi-cell values separately using the Kolmogorov-Smirnov Two-Sample Test (Massey, 1952). Bell-shaped storm values of ΔT_{500} , veering in the subcloud layer, mean wind in the subcloud layer, and shear in the cloud layer were found to differ from the multi-cell storm values at the 99, 90, 95, and 95% confidence level respectively. That is, one could state with that degree of confidence that the values came from different populations. When comparing bell-shaped storm values to supercell values, the test indicated no significant reason to believe that the values did not come from the same population.

Hodographs of vertical wind profiles for each bell-shaped storm case are shown in Figs. 26 through 36. For each case, the amount of turning (θ) with height (H) was determined from the surface up to the point where the hodograph became unidirectional or reversed its direction of turning. These values along with the ratio $\frac{\theta}{H}$ for bell-shaped storm cases are shown in Table 5. The same parameters for supercell cases documented by several authors are shown in Table 6. From the tables, a considerable range of values for both θ and H can be seen. However, the ratio $\frac{\theta}{H}$ was remarkably similar in both tables, the average being 26.0 deg km^{-1} for bell-shaped storms and 27.4 deg km^{-1} for supercell storms.

The data show that bell-shaped storms form in an environment similar to that of supercells. Could the bell-shaped storms in fact be a type of supercell with different characteristics due to their formation near a dryline? Kessler (1969) discusses thunderstorm morphology in relation to updraft speed and water content. Fig. 37 from his work shows profiles of average condensed water in an updraft in relation to maximum updraft speed. He notes that a given value of buoyancy should produce a much stronger updraft in a dry than in a moist atmosphere. This is because the dry atmosphere will produce less water loading to slow the updraft. Kessler also shows that an updraft of 15 m s^{-1} is strong enough to prevent rain from reaching the ground below the updraft. This is consistent with the reports of apparently strong updrafts and rain-free cloud bases in bell-shaped storm cases.

Kessler's strong updraft model also shows a distribution of water substance suggestive of the radar vault in the bell-shaped storm described by Browning (1965). A vault is also implied by the echo overhang reported in the 4 June 1973 storm. No vertical radar observations are available for other bell-shaped storms but the presence of a vault seems likely. Other radar observations of vaults have been shown to be updraft vaults by Marwitz, et al., (1969). Measurements from an instrumented aircraft con-

firmed that organized updrafts were at the base of the vaults.

Kessler's model also shows that strong updrafts are favorable to hail production. Bell-shaped storms have been prolific hail producers.

The following general statements can be made about the bell-shaped storms of this study:

1. They formed in a highly unstable environment ahead of a dryline, often near but south of a dryline/front intersection.

2. A strong upper-level disturbance was not required to trigger the storms.

3. They formed as isolated cells, often to the south of a broken line of existing storms (some of which may have been supercells), and often continued as isolated cells for several hours.

4. Their environment was significantly different than that of the multi-cell storms they were compared with.

5. Their environment was not significantly different than that of the supercell storms they were compared with.

6. An intense updraft (and no downdraft produced by water loading) may give the storms many of their physical characteristics.

The models in Figs. 38 through 41 were constructed to represent major features of the environment in which bell-shaped storms occur. Considerable use was made of the data in Tables 1 and 2 to make the models as representative as possible. In Figs. 38 and 39, an effort was made to preserve typical moisture and temperature profiles and also to realistically represent the changes that occur from morning to afternoon (strong low-level heating, breaking of the inversion, and mid-level cooling). The model hodograph in Fig. 40 was constructed to preserve both the depth and degree of low-level turning of the winds, and the total wind shear typical of that seen in bell-shaped storm environments. Some smoothing was done to construct the surface features shown in Fig. 41. However, the pressure pattern and the orientation of the front and dryline are realistic. Given the conditions shown in these models, a bell-shaped storm might be expected to form in south-central Oklahoma just ahead of the dryline.

CHAPTER V

RECOMMENDATIONS FOR FURTHER STUDY

The large scale fields of moisture and wind have only been touched on in this study. The relationship of the synoptic scale vertical motion field to storm development should be investigated. The large scale fields of vorticity and divergence would also be of interest. Even then, the synoptic scale is only a beginning in understanding the nature of bell-shaped thunderstorms. Mr. L.R. Lemon (formerly of NSSL and NSSFC) has commented that these are "bare-bones" storms (because of their weak appearance compared to supercells). It is clear that standard, synoptic-scale observations are not enough to define what really takes place in and around them. They will have to be studied, as supercells have been, by special soundings, Doppler and conventional radar, surface observations, and aircraft. Coincident time-lapse photography and multiple-Doppler observations should produce some interesting results. Use of chaff may be necessary for updraft measurements into the vault since reflectivity on the order of 20 dBZ or less can be expected (Browning and Foote, 1976; Marwitz, 1970).

Given the proper initial conditions, perhaps a numerical model could produce a bell-shaped storm. Recommendations at this point would be to use a hodograph that turns clockwise with height, and a highly unstable sounding. See Figs. 39 and 40 for suggested sounding and hodograph.

BIBLIOGRAPHY

- Bluestein, H.B., J. McGinley, D. Bowman, D. Carmichael, D. Engles, M. Jain, C. Kessinger, B. Moyer, E. Rasmussen and D. Rusk, 1978: A contribution to the severe storms intercept project - 1978. Final Report, USDC NOAA 04-78-B01-11, School of Meteorology, University of Oklahoma, Norman, 66 pp.
- Brown, R.A., 1976: The Union City, Oklahoma tronado of 24 May 1973. NOAA Tech Memo. ERL NSSL-80, Norman, 235 pp.
- Browning, K.A., 1965: A family outbreak of severe local storms - a comprehensive study of the storms in Oklahoma on 26 May 1963. Part I, ed. K.A. Browning, AF Cambridge Research Lab Special Reports, No. 32, 346 pp.
- _____, 1977: The structure and mechanisms of hail storms. Hail: A Review of Hail Science and Hail Suppression. Met. Monographs, No. 38, 1-43.
- _____, and G.B. Foote, 1976: Airflow and hail growth in supercell storms and some implications for hail suppression. Quart. J. R. Meteorol. Soc., 102, 499-533.
- _____, and R.J. Donaldson, Jr., 1963: Airflow and structure of a tornadoic storm. J. Atmos. Sci., 20, 533-545.
- Burgess, D.W., R.P. Davies-Jones, 1979: Unusual tornadic storms in eastern Oklahoma on 5 December 1975. Mon. Wea. Rev., 107, 451-457.
- Davies-Jones, R.P., and D.W. Burgess and L.R. Lemon, 1976: An atypical tornado-producing cumulonimbus. Weather, 31, 366-347.

- Fawbush, E.J. and R.C. Miller, 1954: The types of air masses in which North American tornadoes form. Bull. Amer. Meteor. Soc., 35, 154-165.
- Fujita, T.T., 1959: A detailed analysis of the Fargo tornadoes of 20 June 1957. Tech. Rep. No. 5, Severe Local Storms Project, Univ. of Chicago, 29 pp.
- Galway, J.G., 1956: The lifted index as a predictor of latent instability. Bull. Amer. Meteor. Soc., 37, 528-529.
- Heymsfield, G.M., 1978: Kinematic and dynamic aspects of the Harrah tornadic storm analyzed from dual-Doppler radar data. Mon. Wea. Rev., 106, 233-254.
- Kessinger, C., and H. Bluestein, 1979: The role of deformation at the dryline/front intersection. Preprints, 11th Conference on Severe Local Storms, Kansas City, Amer. Meteor. Soc., 91-95.
- Kessler, E., 1969: On the continuity of water substance in atmospheric circulations. Met. Monographs, 10, No. 32, 84 pp.
- Klemp, J.B., and R. Wilhelmson, 1978a: The simulation of three-dimensional convective storm dynamics. J. Atmos. Sci., 35, 1070-1096.
- _____, and _____, 1978b: Simulations of right and left moving storms through storm splitting. J. Atmos. Sci., 35, 1097-1100.
- Lemon, L.R., 1976: Tornadic storm evolution: Vortex valve hypothesis. The Union City, Oklahoma Tornado of 24 May 1973. R.A. Brown, Editor. NOAA Tech. Memo. ERL NSSL-80, Norman, 235 pp.
- Maddox, R.A., L.R. Hoxit, and C.F. Chappell, 1980: A study of tornadic thunderstorm interactions with thermal boundaries. Mon. Wea. Rev., 108, 322-336.
- Marwitz, J.D., 1972a: The structure and motion of severe hailstorms. Part I: Supercell storms. J. Appl. Meteor., 11, 166-179.

- _____, 1972b: The structure and motion of severe hailstorms. Part II: Multi-cell storms. J. Appl. Meteor., 11, 180-188.
- _____, A.H. Auer, Jr., and D.L. Veal, 1972: Locating the organized updraft on severe thunderstorms. J. Appl. Meteor., 11, 236-238.
- _____, J.R. Middleton, A.H. Auer, Jr., and D.L. Veal, 1970: The dynamics of updraft vaults in hailstorms as inferred from the entraining jet model. J. Atmos. Sci., 27, 1099-1102.
- Massey, F.J., 1952: Distribution table for the deviation between two sample cumulatives. Ann. Math. Stat., 23, 435-441.
- Miller, R.C., 1972: Notes on analysis and severe-storm forecasting procedures of the Air Force Global Weather Central. AWS Tech. Rep. 200 (Rev.), Air Weather Service (MAC), USAF, 178 pp.
- Nelson, S.P., 1980: A study of hail production in a super-cell storm using a Doppler derived wind field and a numerical hail growth model. NOAA Tech. Memo. ERL NSSL-89, Norman, 90 pp.
- Ray, P.S., R.J. Doviak, G.B. Walter, D. Sirmans, J. Carter, and B. Bumgarner, 1975: Dual-Doppler observation of a tornadic storm. J. Appl. Meteor., 14, 1521-1530.
- Teqtmeier, S., 1974: The role of the surface sub-synoptic low pressure system in severe weather forecasting. M.S. thesis, School of Meteorology, Univ. of Okla., Norman, 66 pp.

APPENDIX

SYNOPTIC FEATURES FAVORABLE FOR SEVERE THUNDERSTORM DEVELOPMENT

Both dynamic and thermodynamic factors must be considered in forecasting severe thunderstorms. Upper-air soundings should be analyzed for the thermodynamic factors. The dynamic factors are determined by relative strengths and positions of upper-level troughs, jets, and temperature patterns.

A thermodynamically unstable atmosphere is necessary for severe storms. One indicator of stability is the lifted index. A maximum temperature is forecast and an average moisture content in the lowest 3000 ft of the atmosphere is determined. A parcel is then lifted adiabatically to 500 mb. The difference between the 500 mb temperature and the parcel temperature is the lifted index. A lifted index of -2 would be a weak indicator of severe storms, while -6 would be a strong indicator (Miller, 1972). If the moist layer is less than 3000 ft deep, moisture advection is usually required to produce severe storms. Low-level moisture (water vapor mixing ratio) of 8 gm kg^{-1} is a weak indicator, while

12 gm kg^{-1} is strong (Miller, 1972). Of the dynamic factors, Miller ranks positive vorticity advection (PVA) highest. If 500 mb contours cross vorticity lines at more than a 30° angle, PVA is considered strong. Other factors as ranked by Miller are shown in Table 7.

The following general requirements for severe storms is adapted from Browning (1965):

1. A preexisting low-level convergence field and a high-level divergence field is desirable.
2. A surface low pressure area should be present to the west.
3. Warm air and moisture advection at 850 mb.
4. Temperature advection at 700 mb changing from positive before the storms to negative after they begin.
5. A 500 mb trough with cold air advection leading that at 700 mb.
6. A high-level jet just west or northwest of the threat area.
7. A thermodynamically unstable atmosphere.

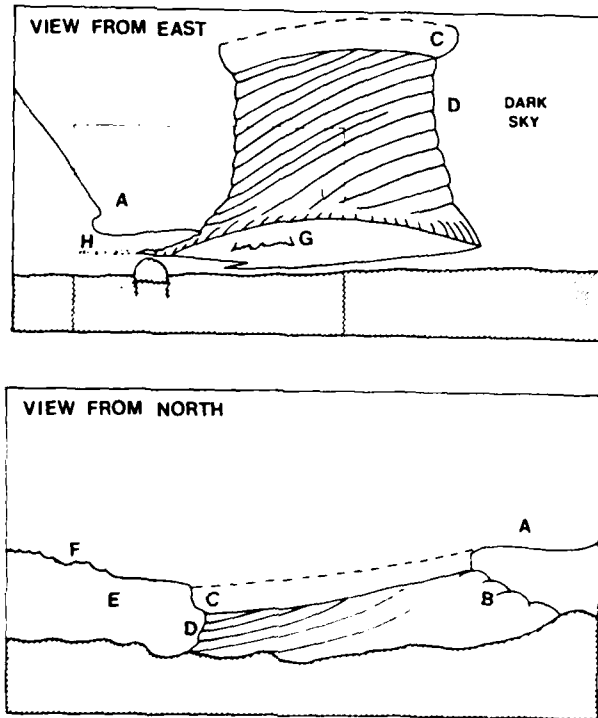


Fig. 8 View from east based on authors' observations from NSSL between 1845 and 1920 CST, and view from north based on G. Gerber's movie taken at 1830 CST from 34 km north of MBG. A - upshear anvil, B - flanking cumulus congestus, C - ring of mid-level cloud, D - rotating cumulonimbus with helical striations, E - virga, rain and hail falling from anvil ahead of bell-shaped cloud, F - downshear anvil and mammatus, G - wall cloud, H - inflow clouds (present intermittently)

Fig. 1. Sketch of the bell-shaped storm of 4 June 1973. (From Davies-Jones *et al.*, 1976).

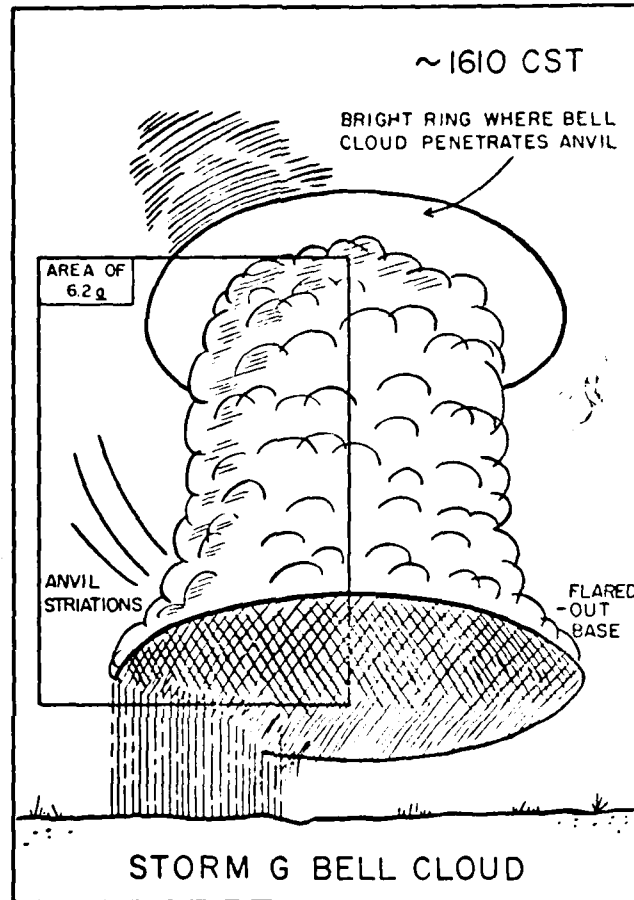


Figure 6. 2b

Figure 6. 2. Figure 6. 2a is a composite of two photographs obtained looking toward the northeast from Location D at 30° and 60° elevation, respectively. It shows the northwest edge of the towering bell-shaped cumulonimbus cloud of Storm G. Figure 6. 2b is a sketch intended to show the approximate shape of the entire cloud. Note that the edge of the bell rises nearly vertically from near the level of its flared base, close to 4000 ft, up to the anvil base, near 28,000 ft. Note also the sharply defined ring of light that surrounds the bell cloud where it penetrates the anvil and the striations within the anvil base itself. The dark cloud in the top right portion of Figure 6. 2a is low-level scud, which is partly obscuring the bell cloud.

Fig. 2. Sketch of the bell-shaped storm of 26 May 1963. (From Browning, 1965).

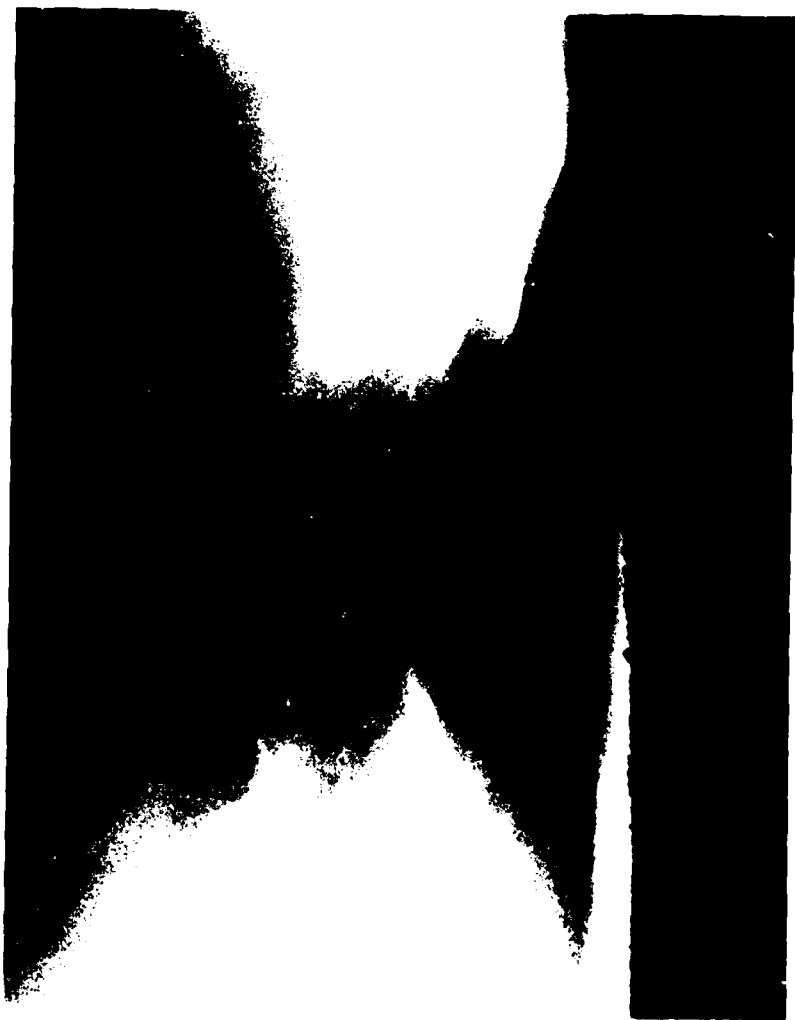


FIG. 3. Photograph of the bell-shaped storm of 16 May 1978,
looking to the west.

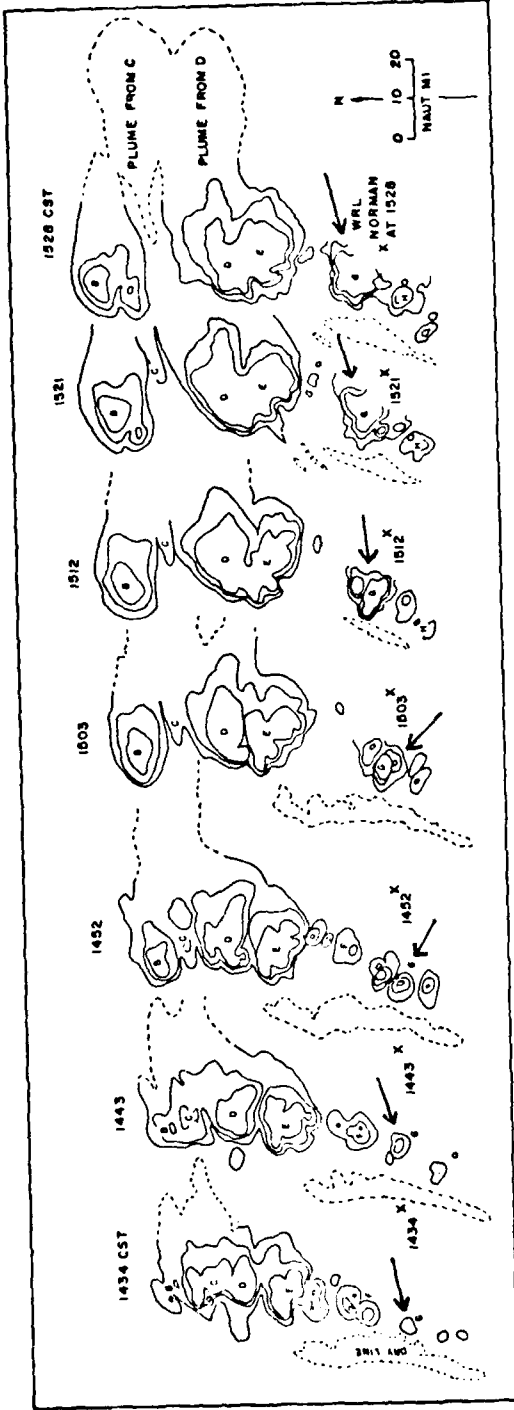


Figure 11.1. The line of storms B through H at roughly 9-min intervals, as seen by the WSR-57 radar at WRL, Norman. The position of the radar, indicated by a cross, is displaced toward the east by distances that are proportional to time. The three solid contours, representing storm echoes at an elevation of 20, are for $10 \log Z_e = 3, 21, 33$, respectively, at a range of 30 naut. mi., where Z_e is the equivalent reflectivity factor in $\text{mm}^6 \text{m}^{-3}$. The dashed contours, representing the dry line, are for $10 \log Z_e = 3$ at 30 naut. mi.; from 1512 onward they are for 20 elevation, whereas before this time they are for 00 elevation and 2 min before the indicated time.

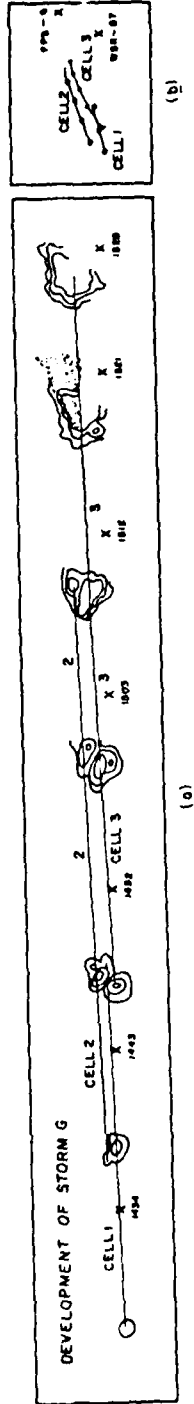


Figure 11.2. (a) Same as Figure 11.1, but showing only the three cells comprising Storm G. Lines are drawn connecting the center of each cell from one time to the next. The shaded area depicted at time 1521 shows the time-integrated extent of hail at the surface due to Storm G during its development phase. (b) Tracks of the centers of the Storm G cells, from Figure 11.2a.

Fig. 5. Radar depiction of storm formation, 26 May 1963. Arrow indicates bell-shaped storm. (From Browning, 1965).

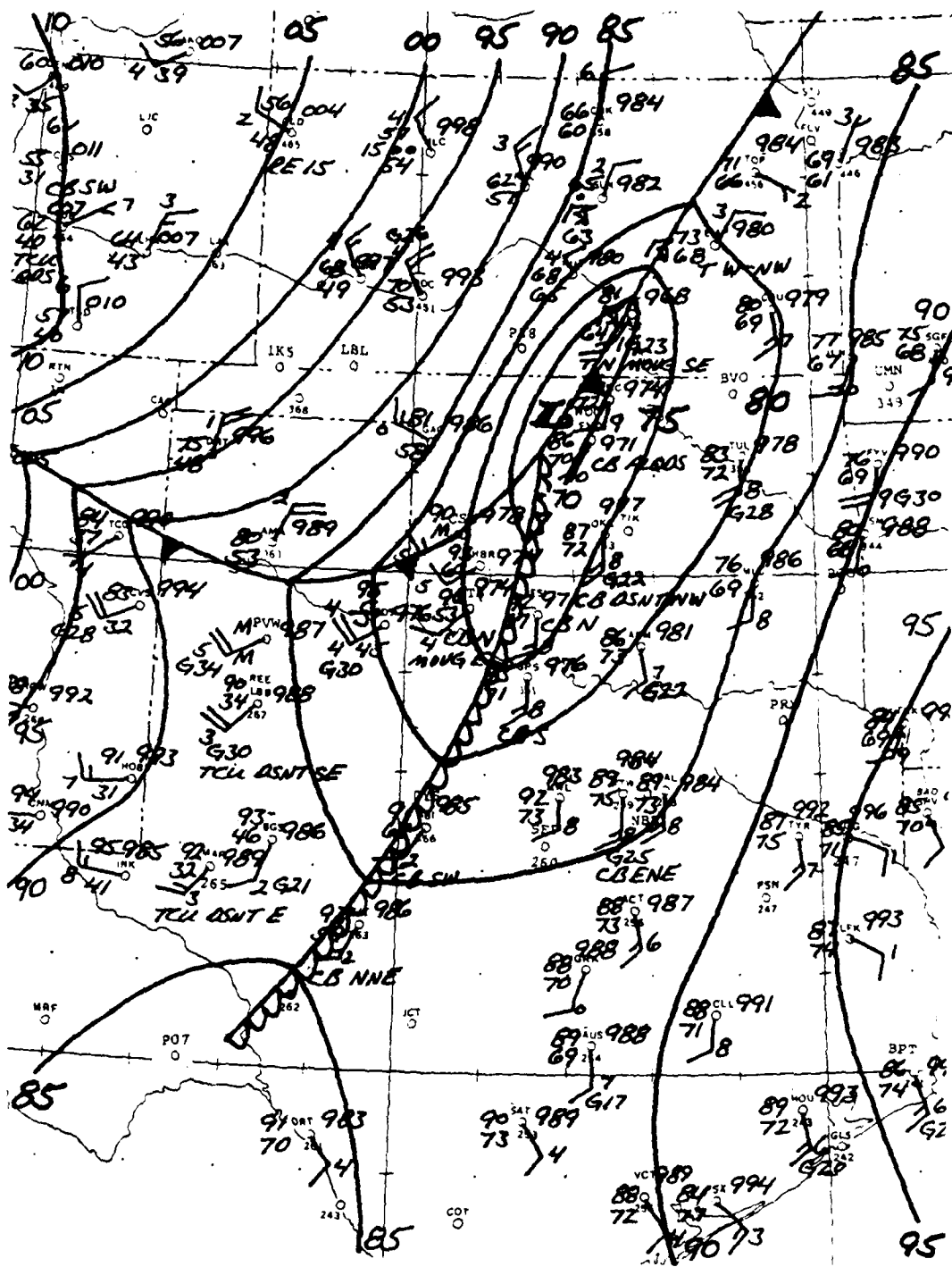


Fig. 6. Surface analysis 1600 CST, 4 June 1973.

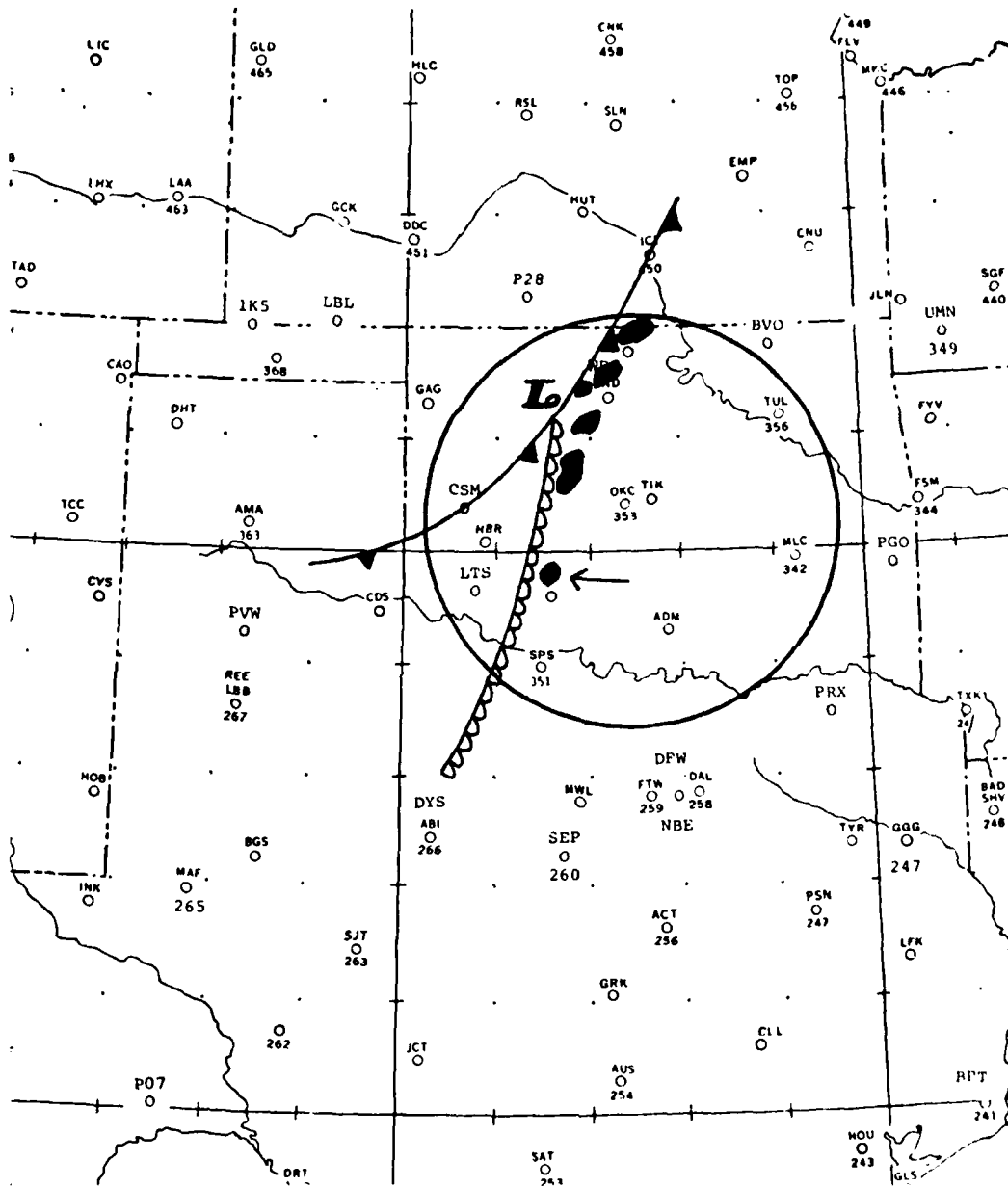


Fig. 7. Radar depiction 1615 CST, 4 June 1973 with 1600 CST surface features. Arrow indicates bell-shaped storm.

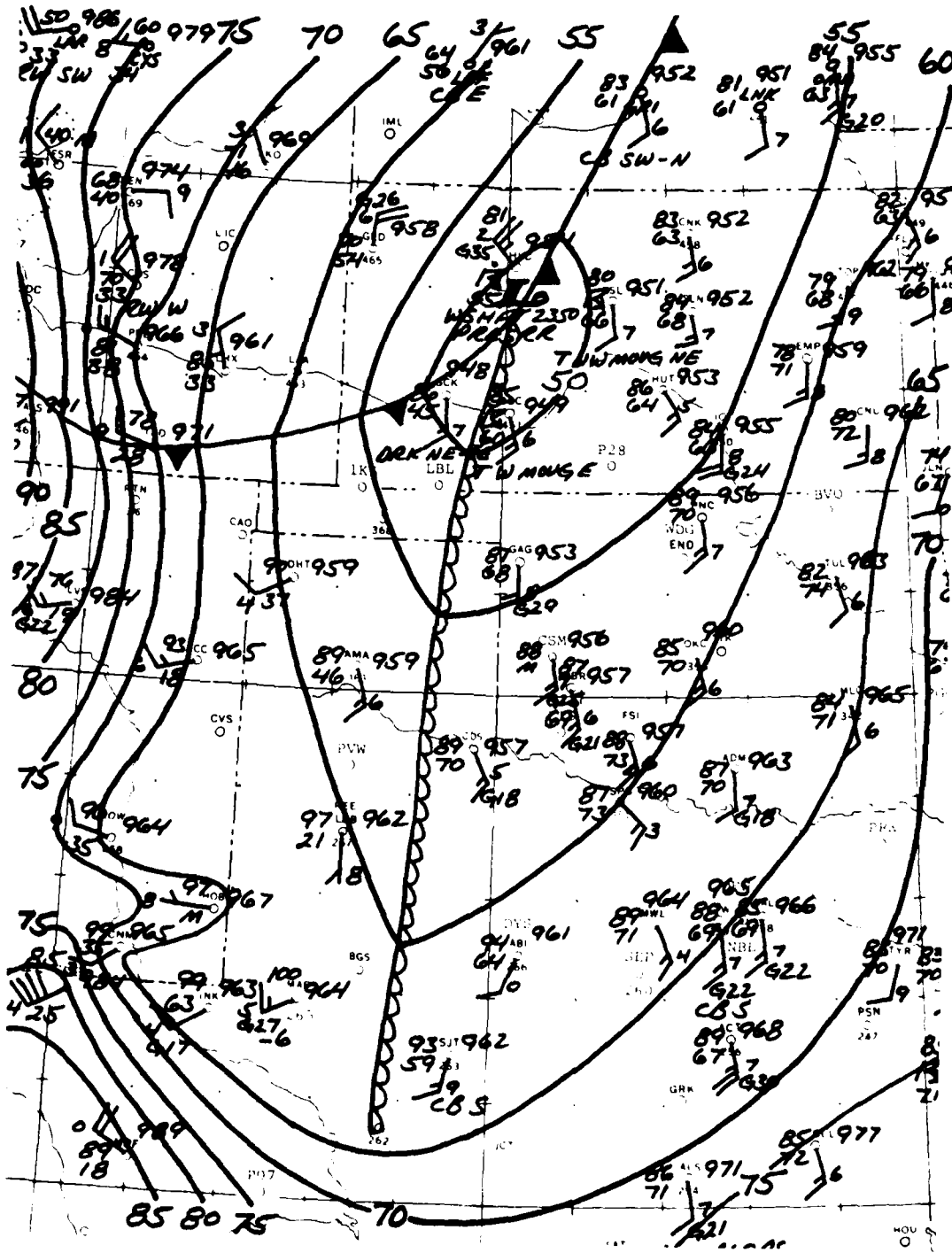


Fig. 8. Surface analysis 1800 CST, 5 June 1974.

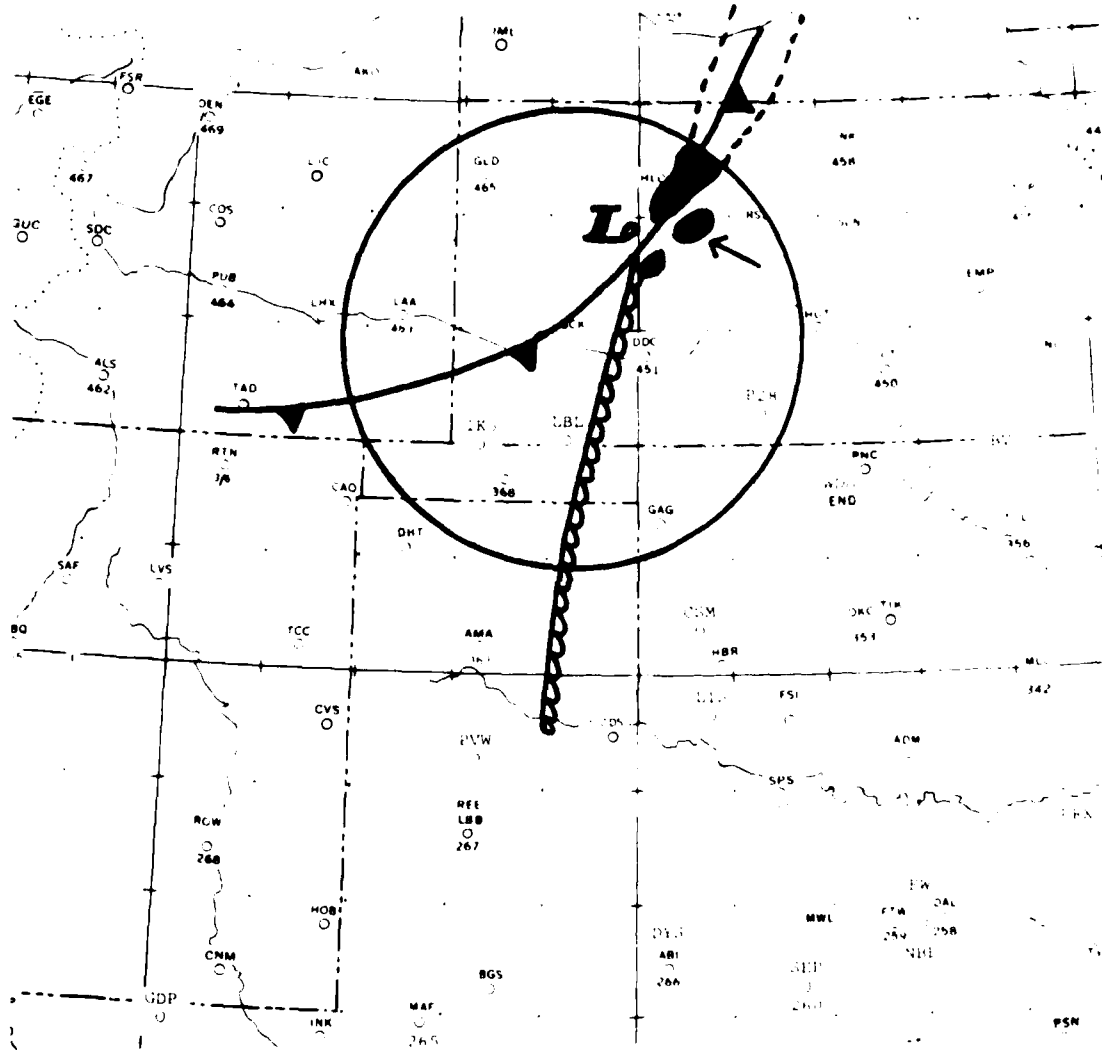


Fig. 9. Radar depiction 1745 CST, 5 June 1974 with 1800 CST surface features. Arrow indicates bell-shaped storm.

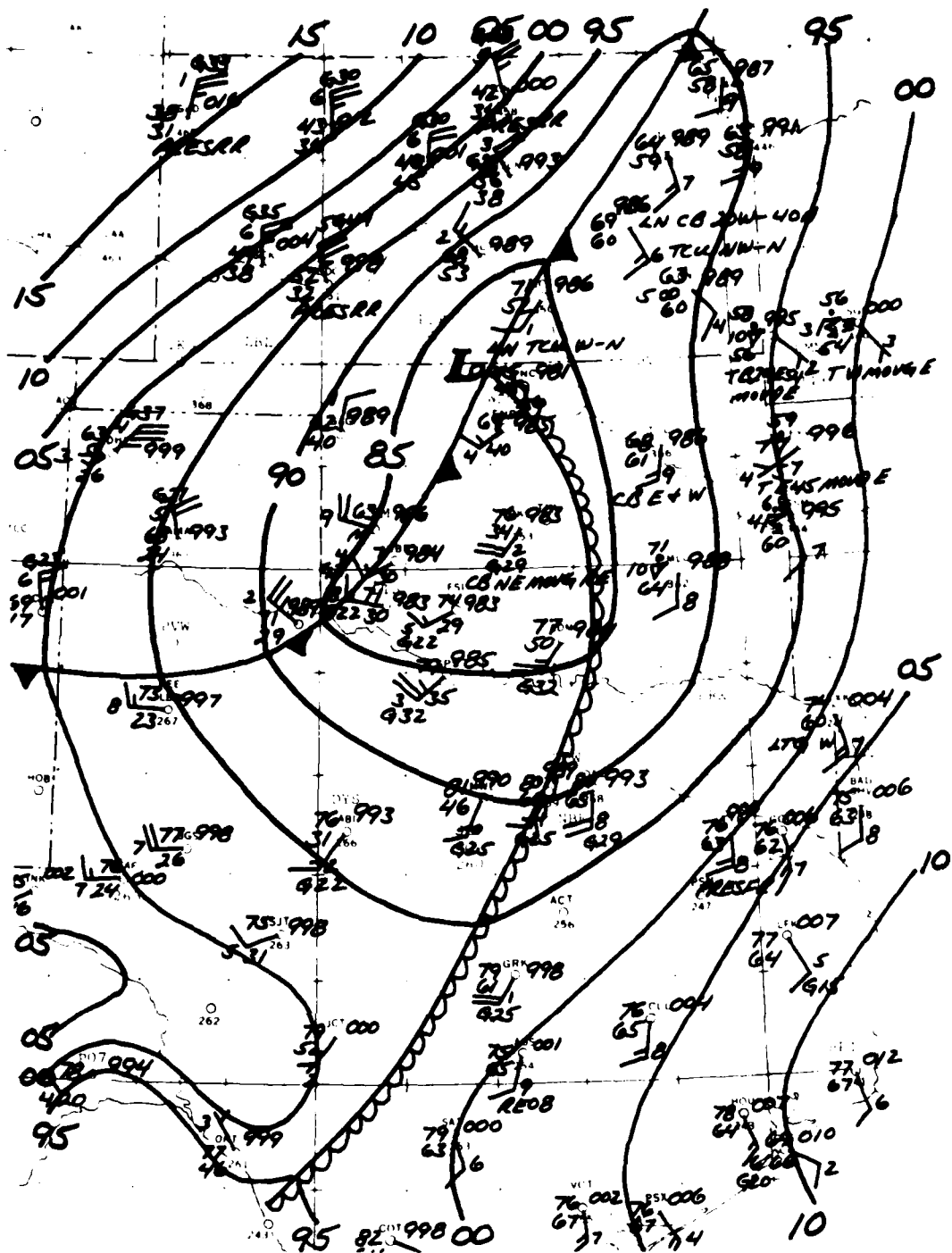


Fig. 10. Surface analysis 1500 CST, 5 December 1975.

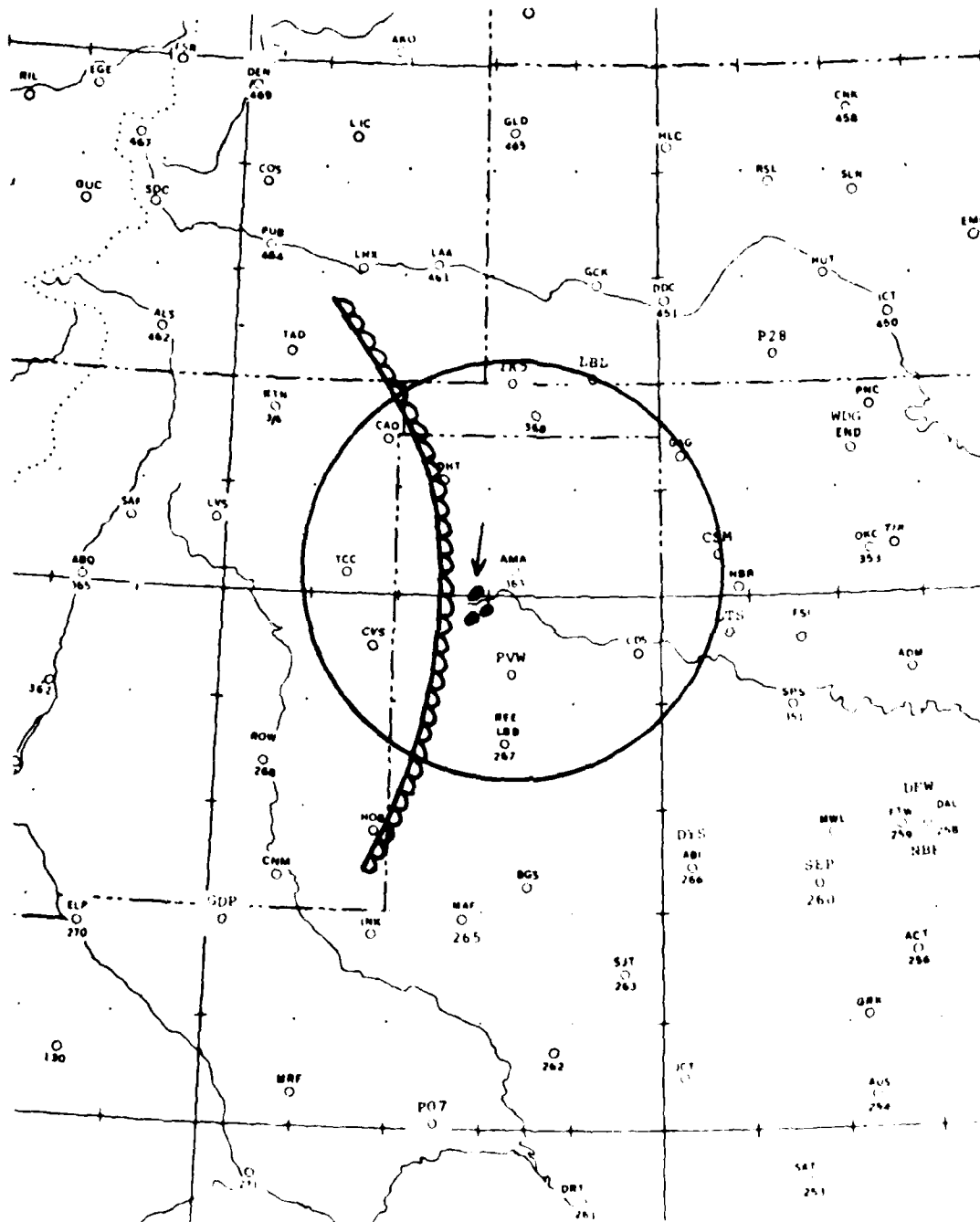


FIG. 13. Radar depiction 1508 CST, 26 April 1976 with 1500 CST surface features. Arrow indicates bell-shaped storm.

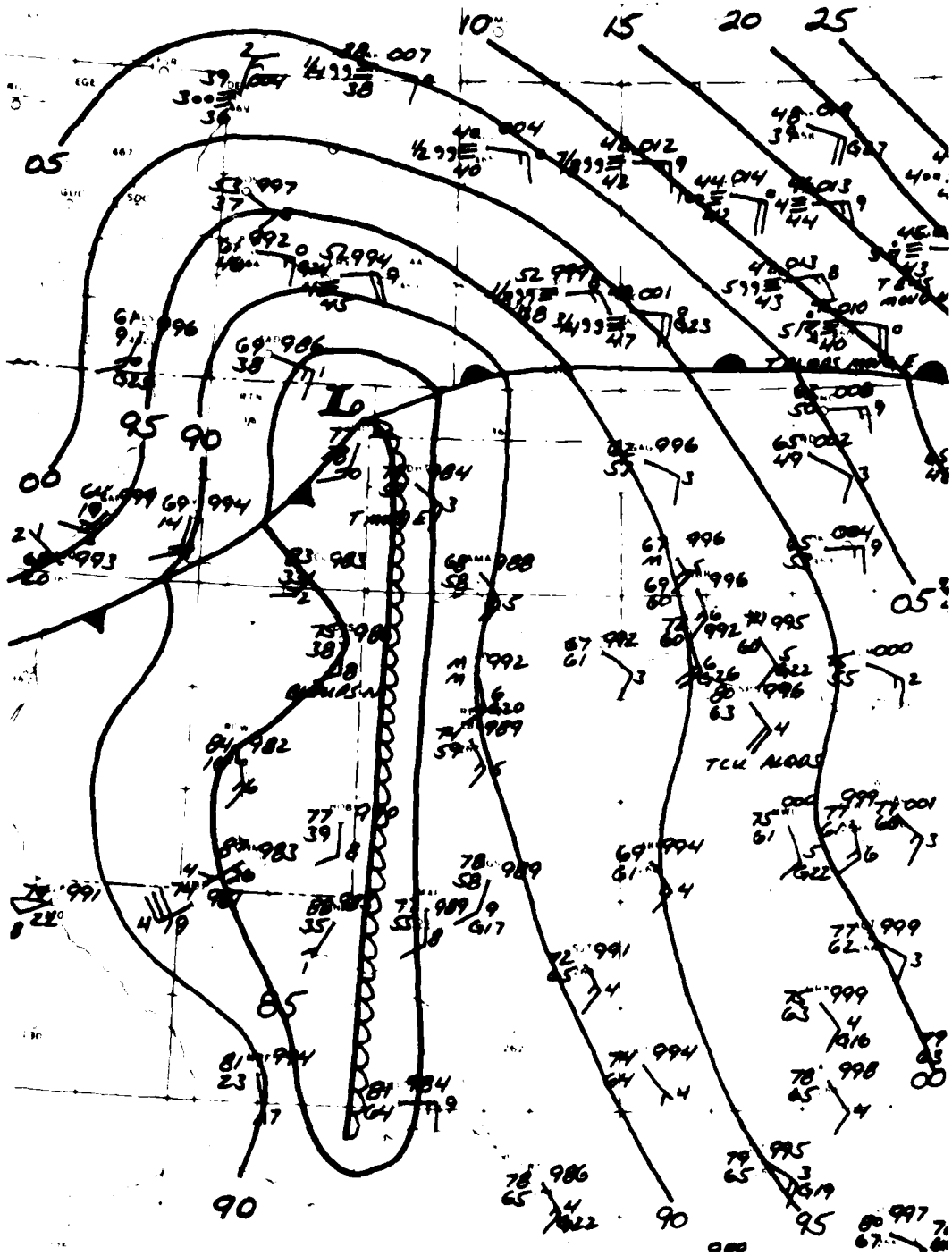


FIG. 14. Surface analysis 1300 CST, 27 April 1976.

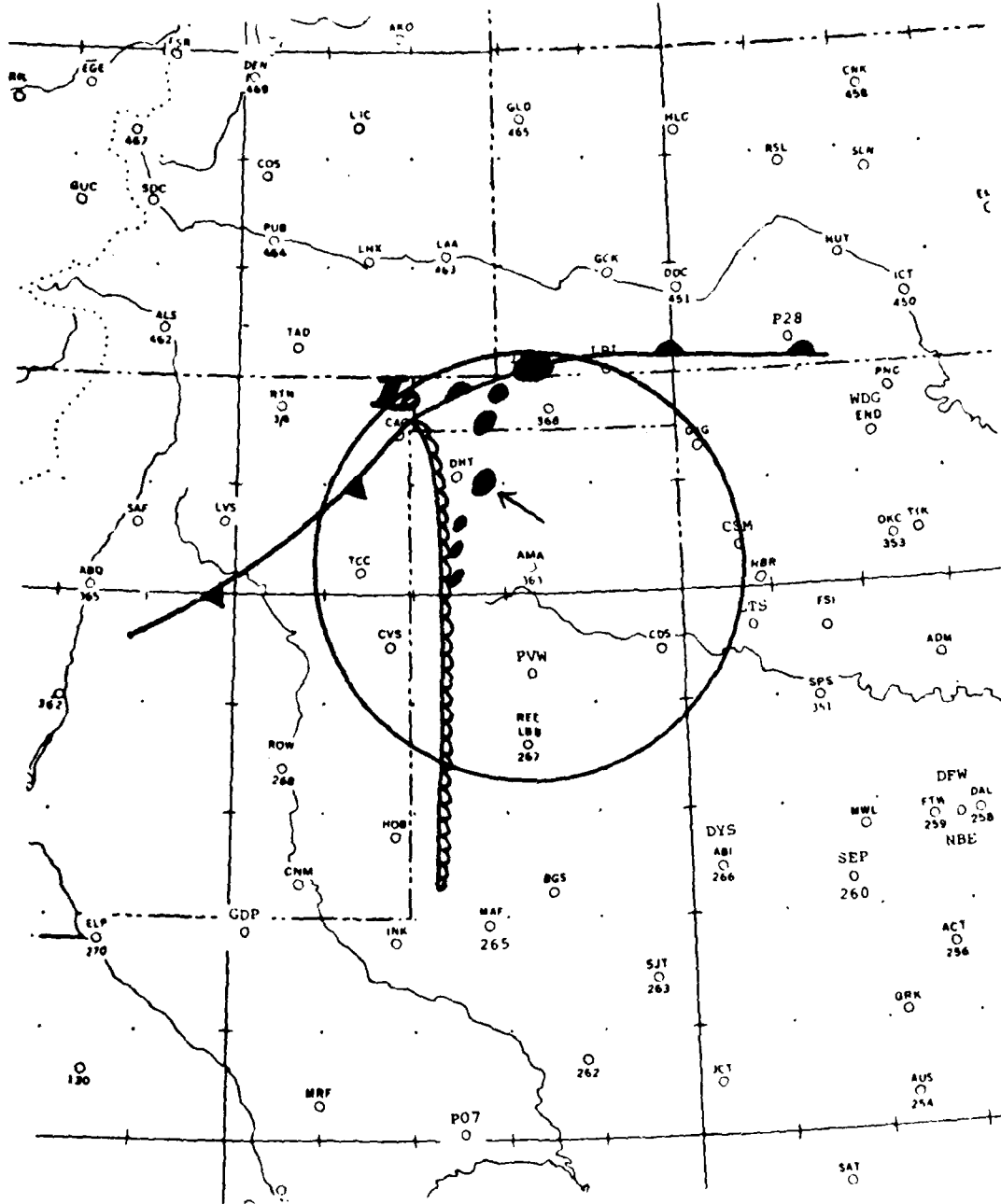


Fig. 15. Radar depiction 1450 CST, 27 April 1976 with 1500 CST surface features. Arrow indicates bell-shaped storm.

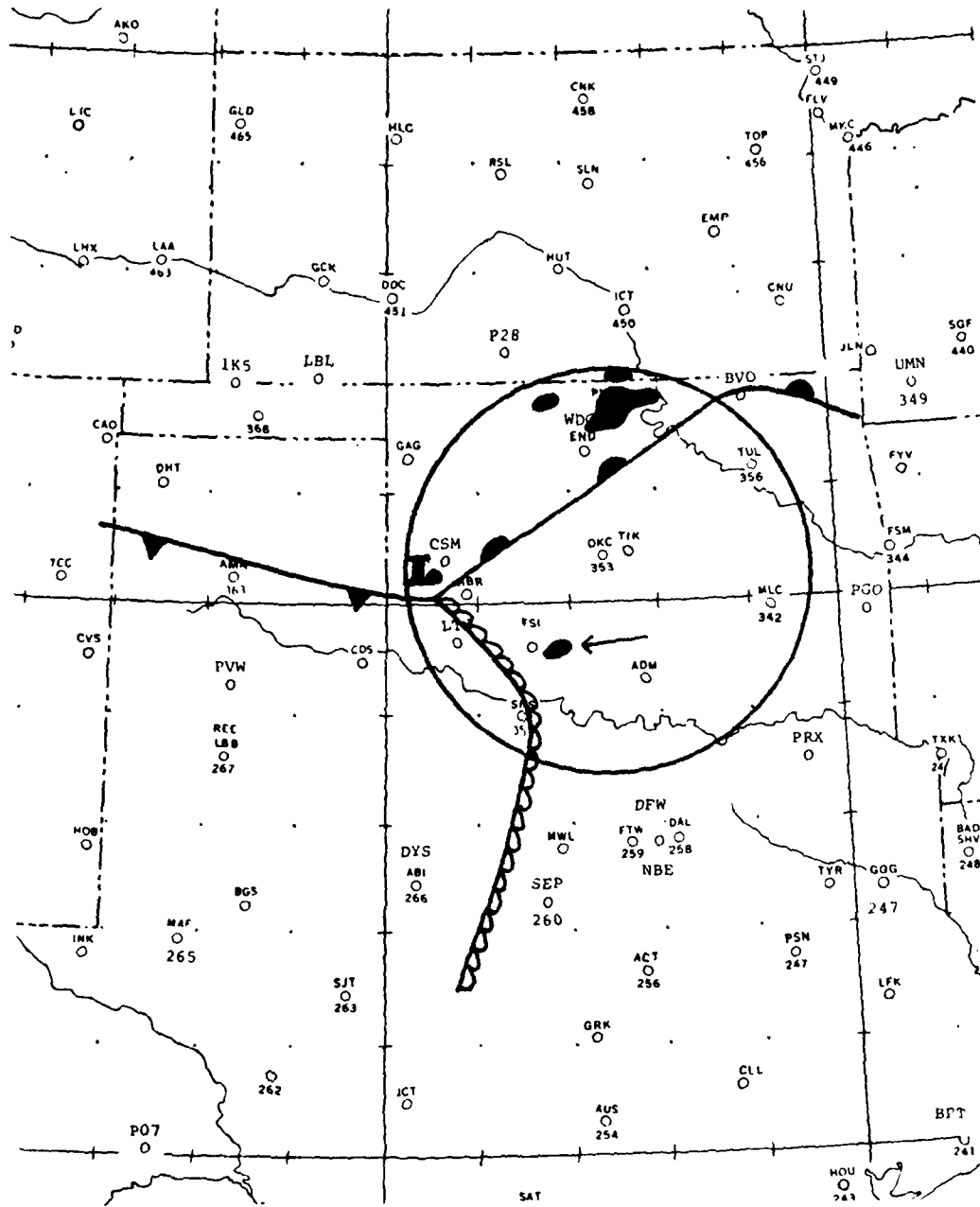


Fig. 17. Radar depiction 1500 CST, 30 April 1978 with 1500 CST surface analysis. Arrow indicates bell-shaped storm.

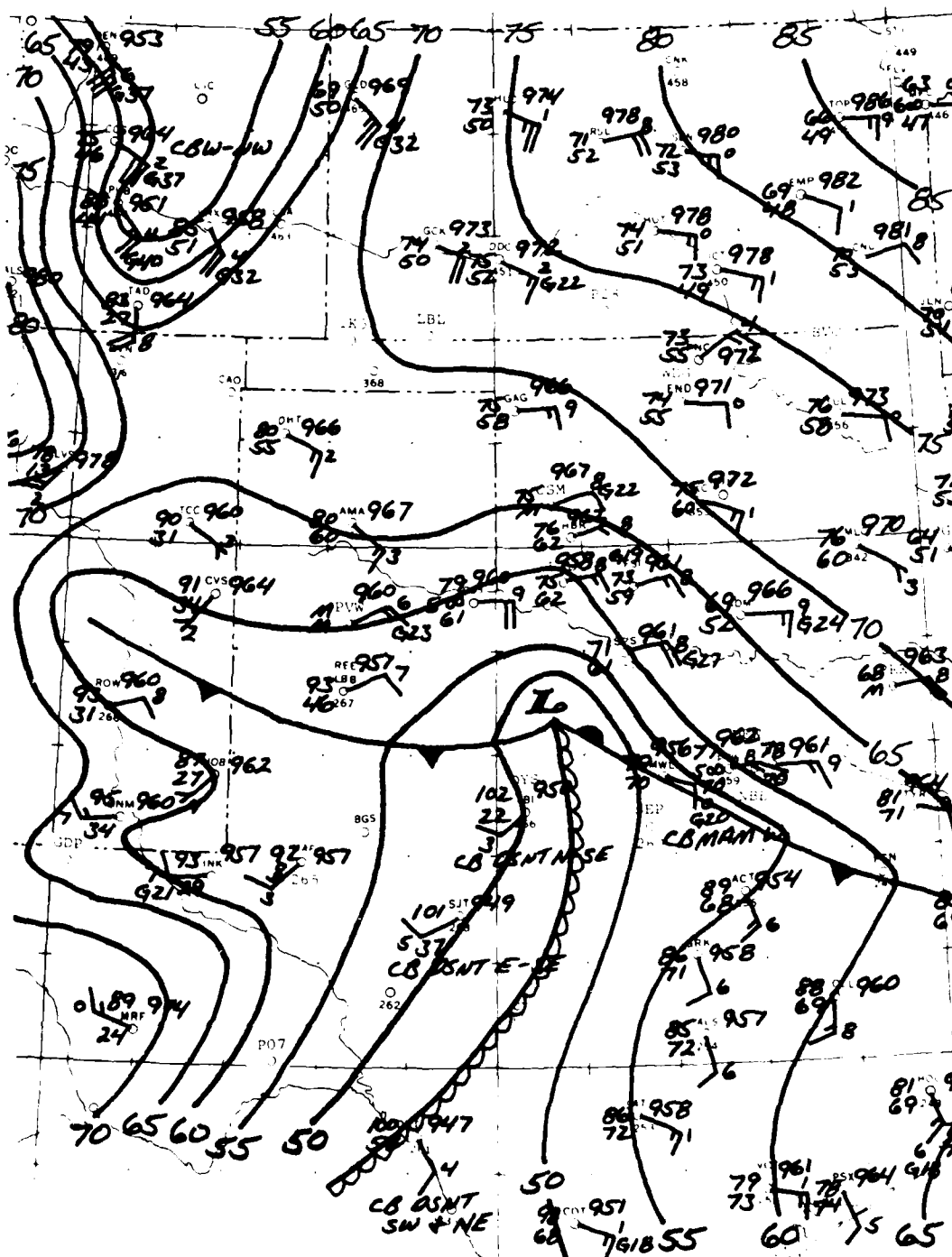


Fig. 18. Surface analysis 1800 CST, 16 May 1978.

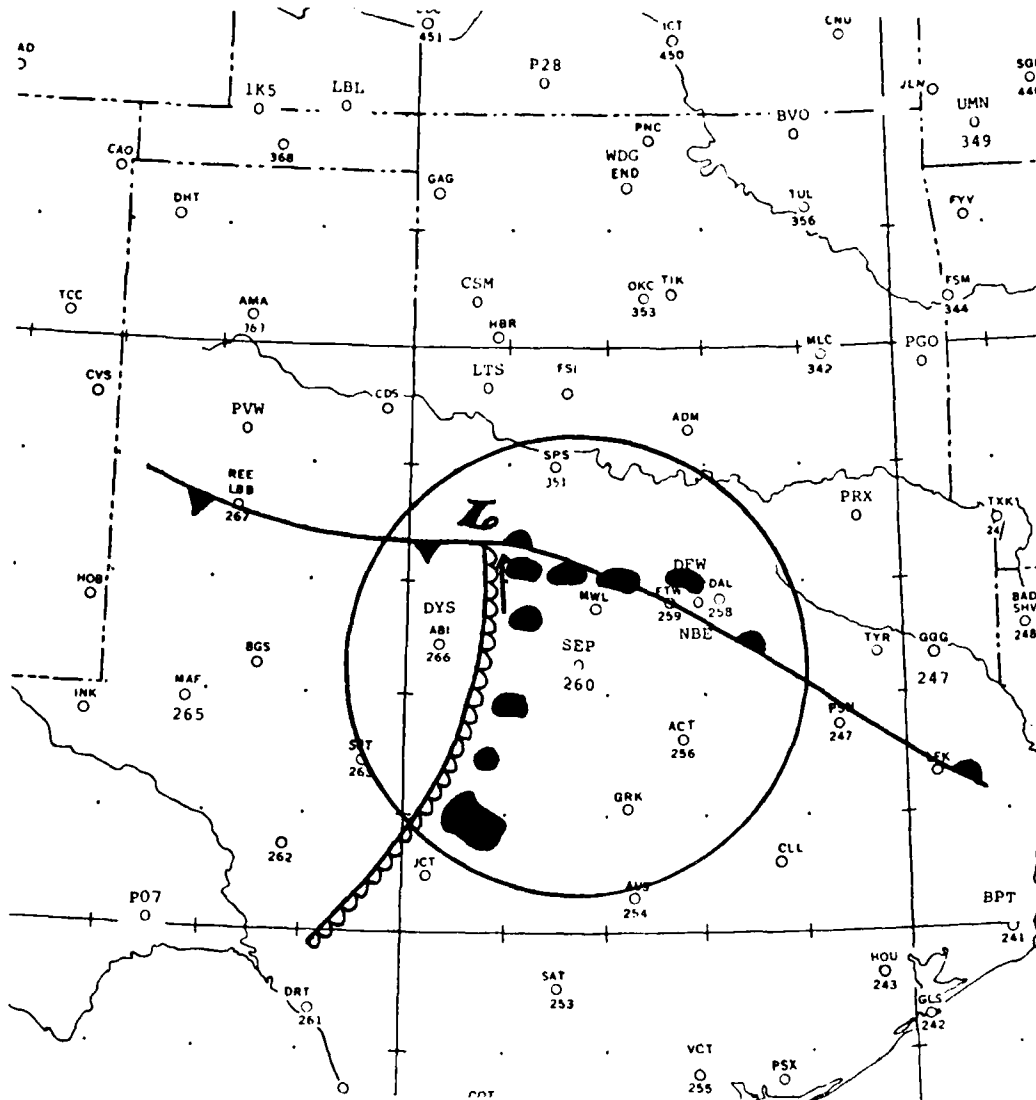


Fig. 19. Radar depiction 1500 CST, 16 May 1978 with 1500 CST surface features. Arrow indicates where bell-shaped storm was observed near 1800 CST when no radar data was available.

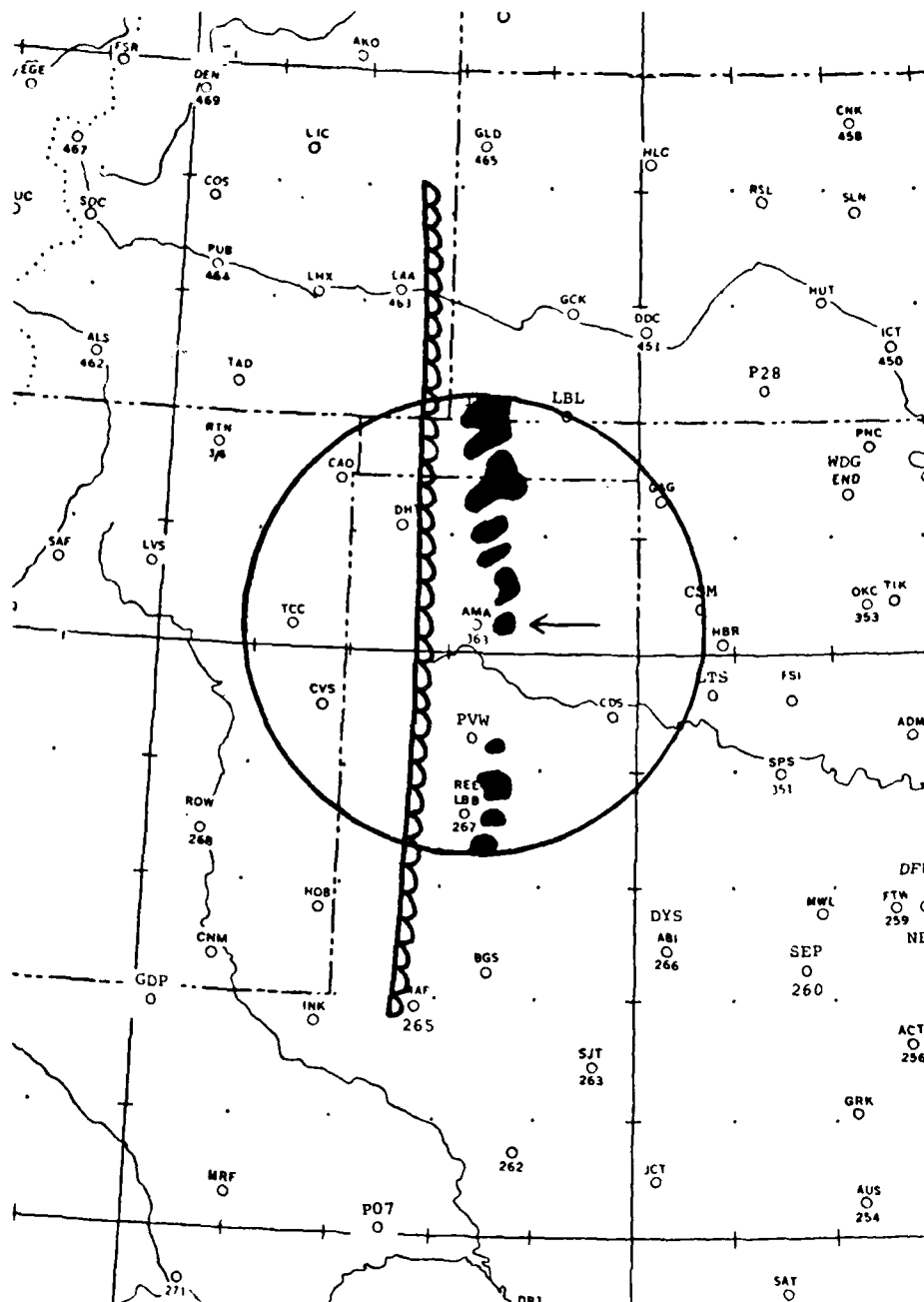


Fig. 21. Radar depiction 1815 CST, 24 May 1978 with 1800 CST surface features. Arrow indicates bell-shaped storm.

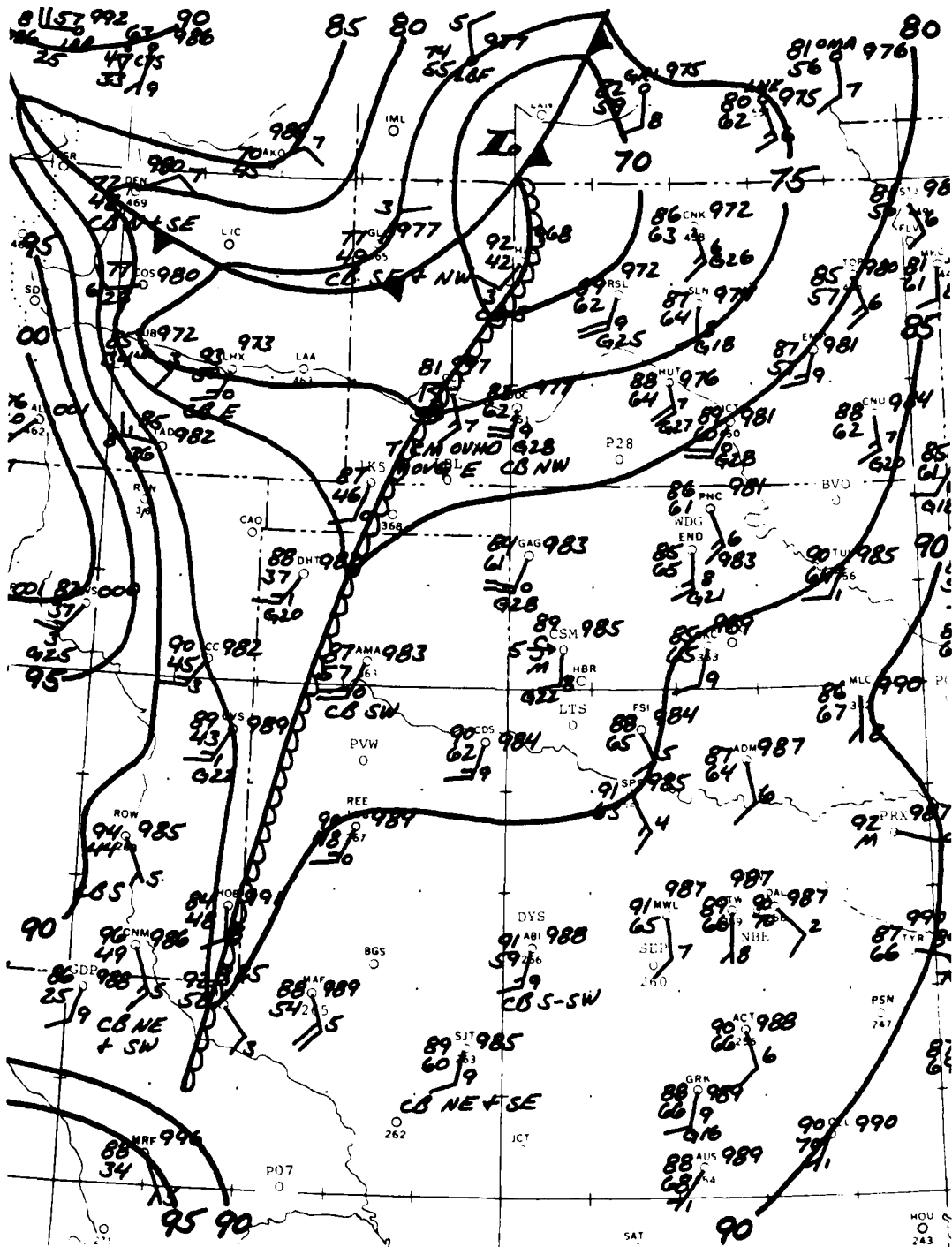


Fig. 22. Surface analysis 1500 CST, 30 May 1978.

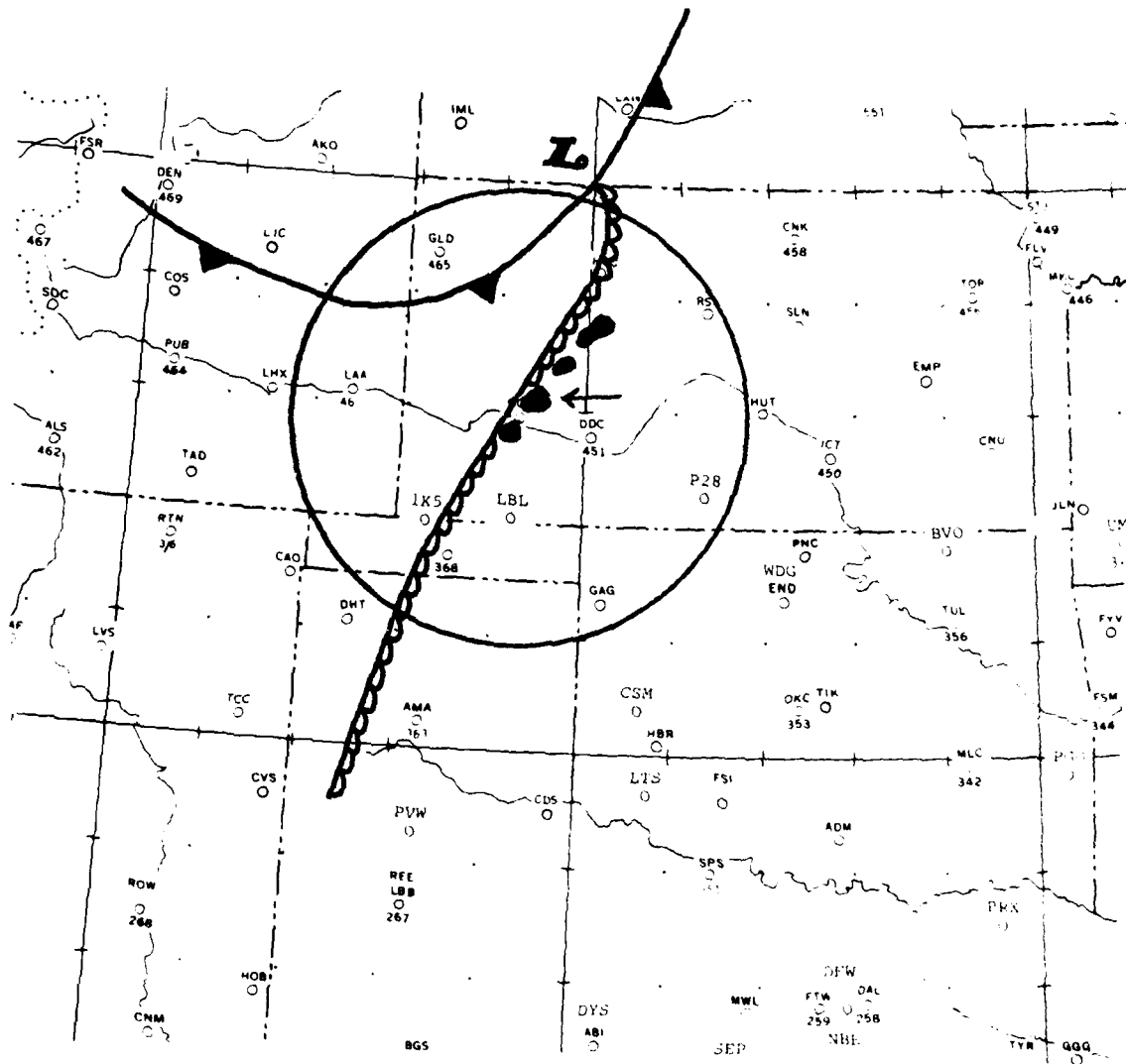


Fig. 23. Radar depiction 1503 CST, 30 May 1978 with 1500 CST surface features. Arrow indicates bell-shaped storm.

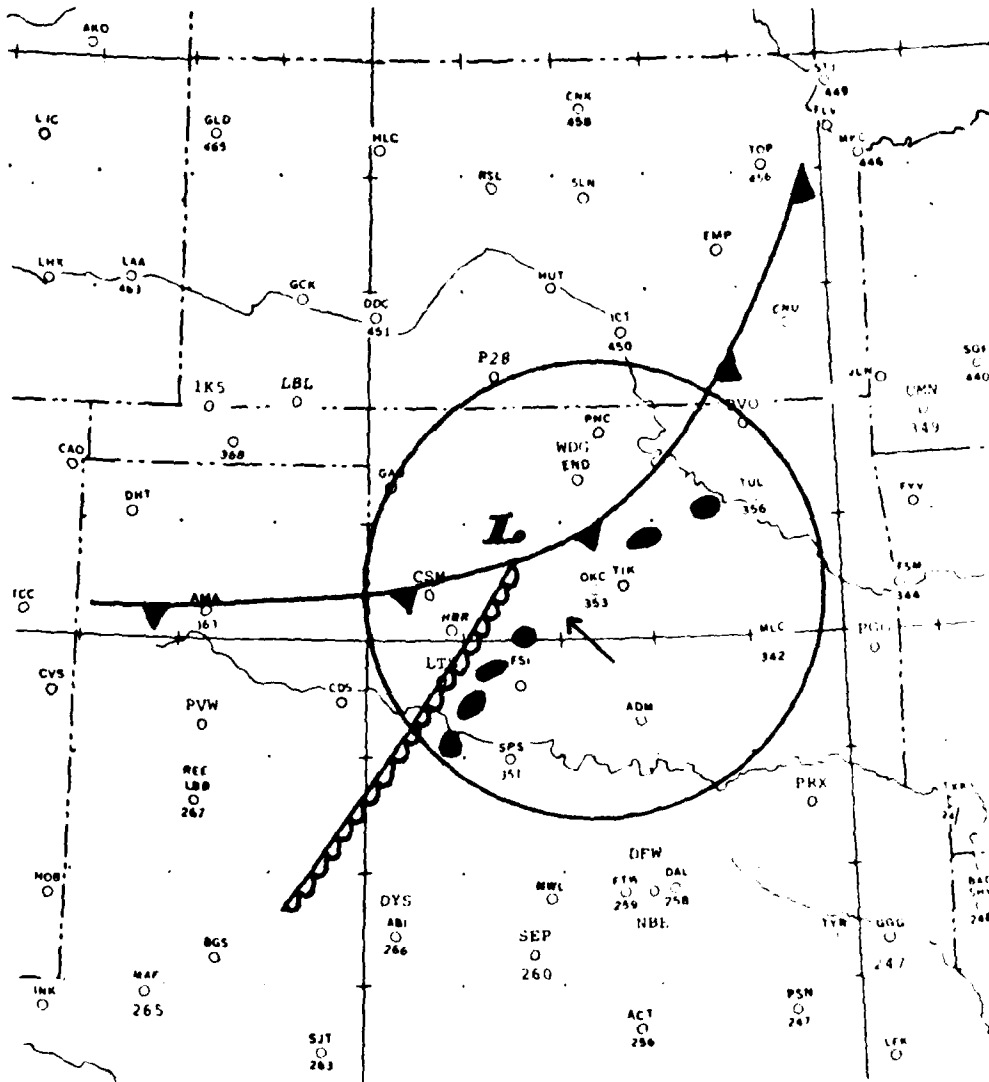


Fig. 25. Radar depiction 1513 CST, 20 June 1979 with 1500 CST surface features. Arrow indicates where bell-shaped storm was observed near 1800 CST when no radar data was available.

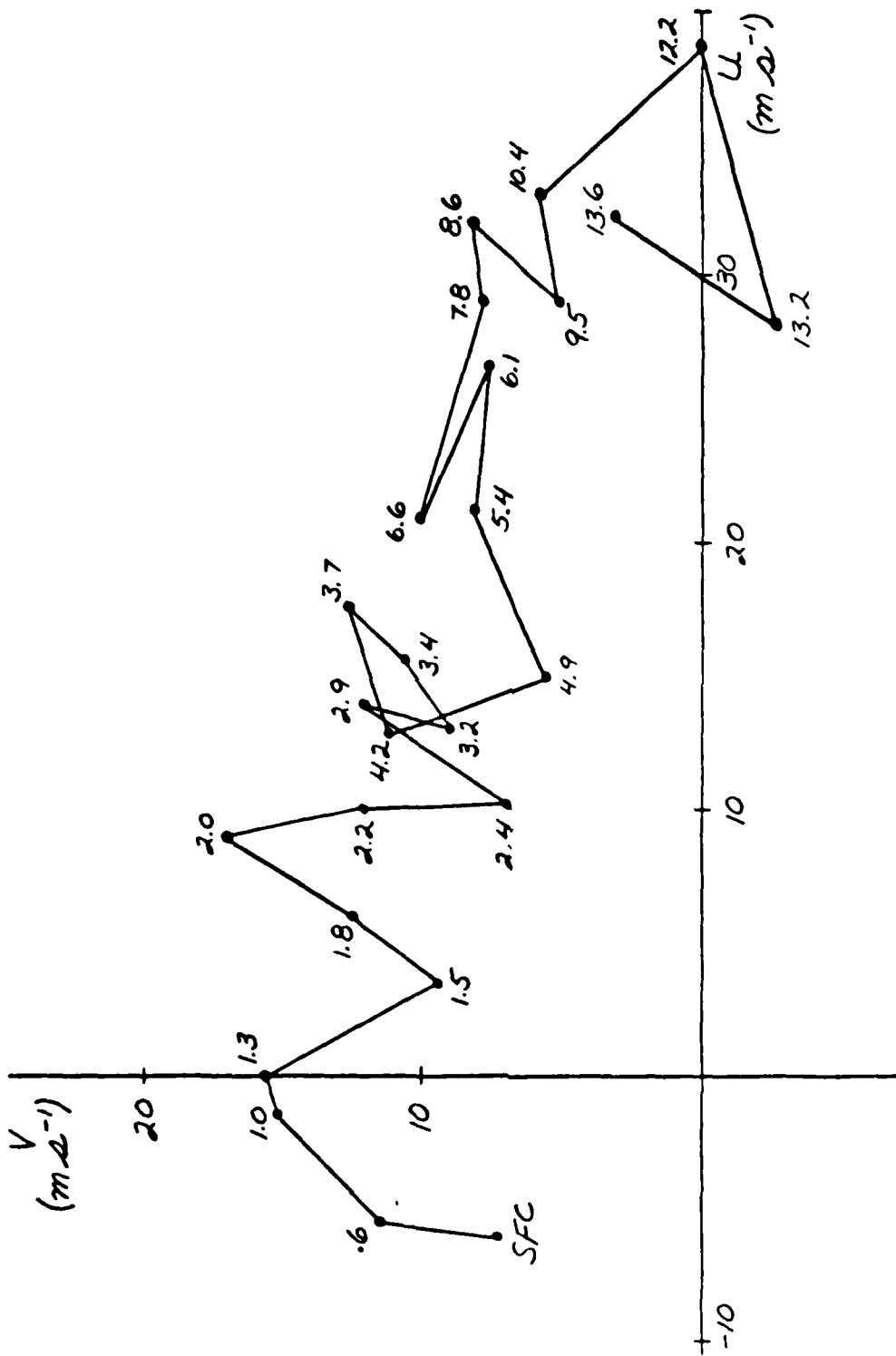


Fig. 26. Hodograph of winds from Oklahoma City sounding 1420 CST, 26 May 1963. Surface wind from near time and location of bell-shaped storm formation. Heights in km.

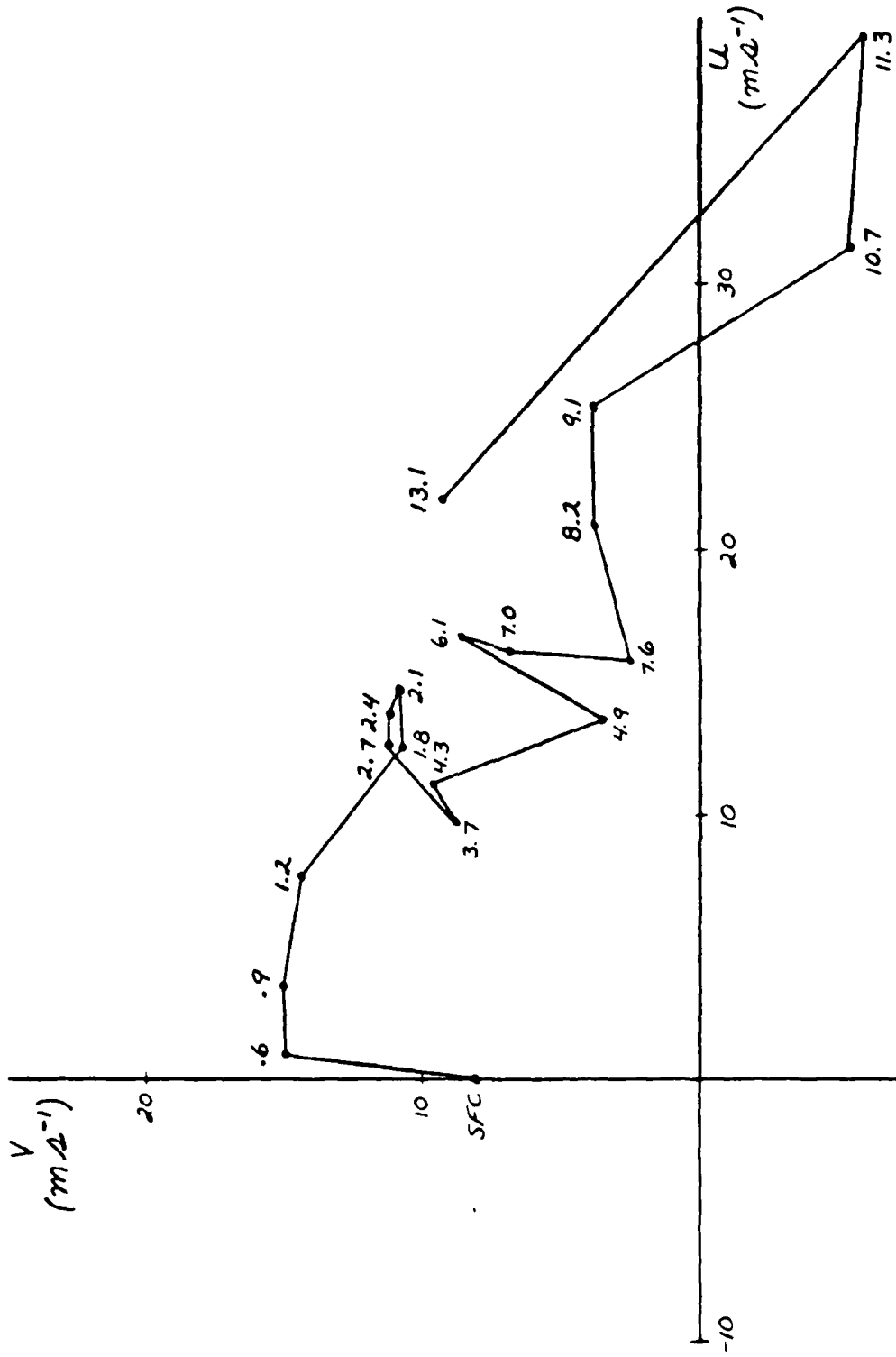


FIG. 27. Composite hodograph of winds from 0600 and 1800 CST, 4 June 1973 soundings at Tinker AFB, OK. Surface wind from near time and location of bell-shaped storm formation. Heights in km.

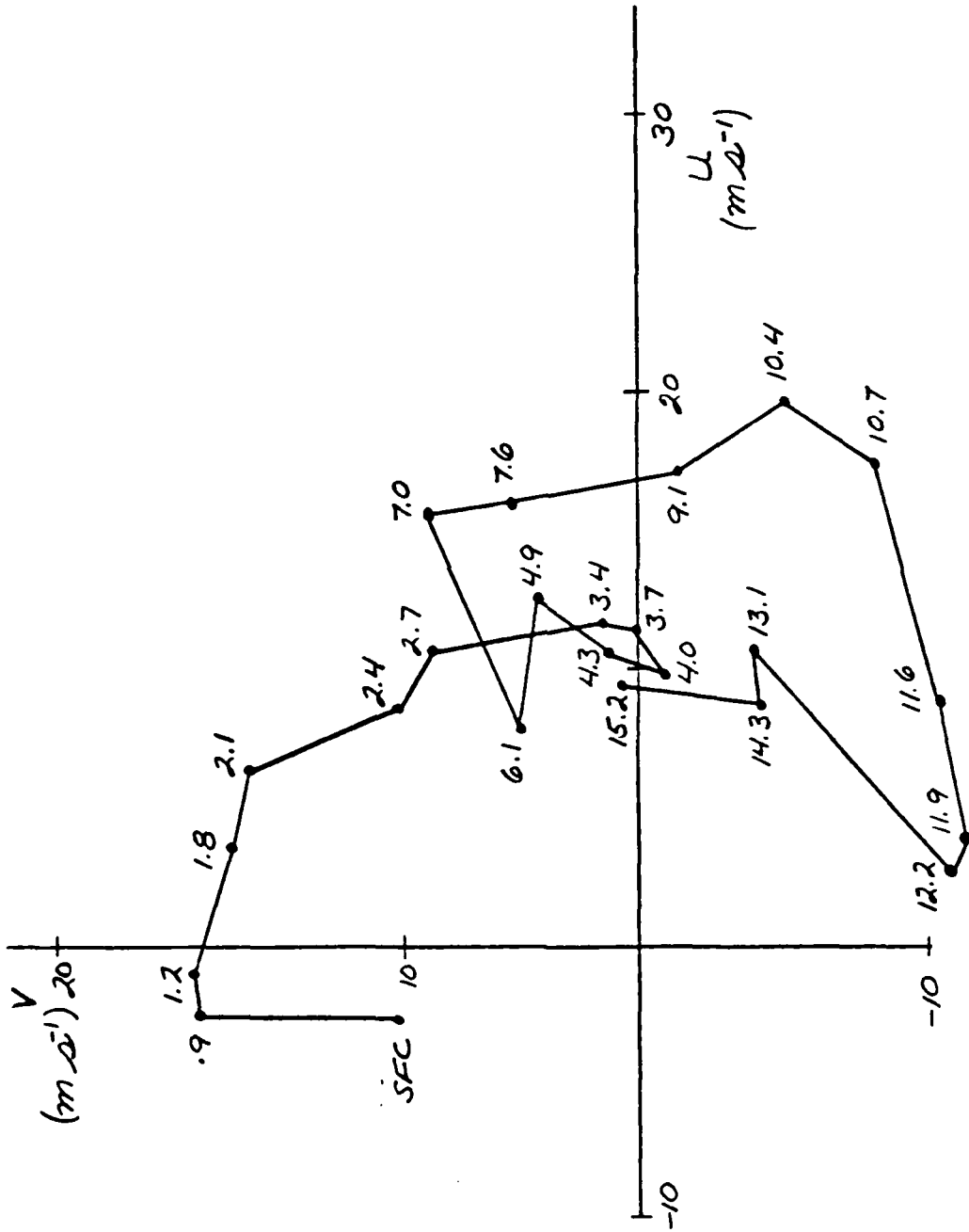


Fig. 28. Hodograph of winds from Dodge City sounding 1800 CST, 5 June 1974. Surface wind from near time and location of bell-shaped storm formation. Heights in km.

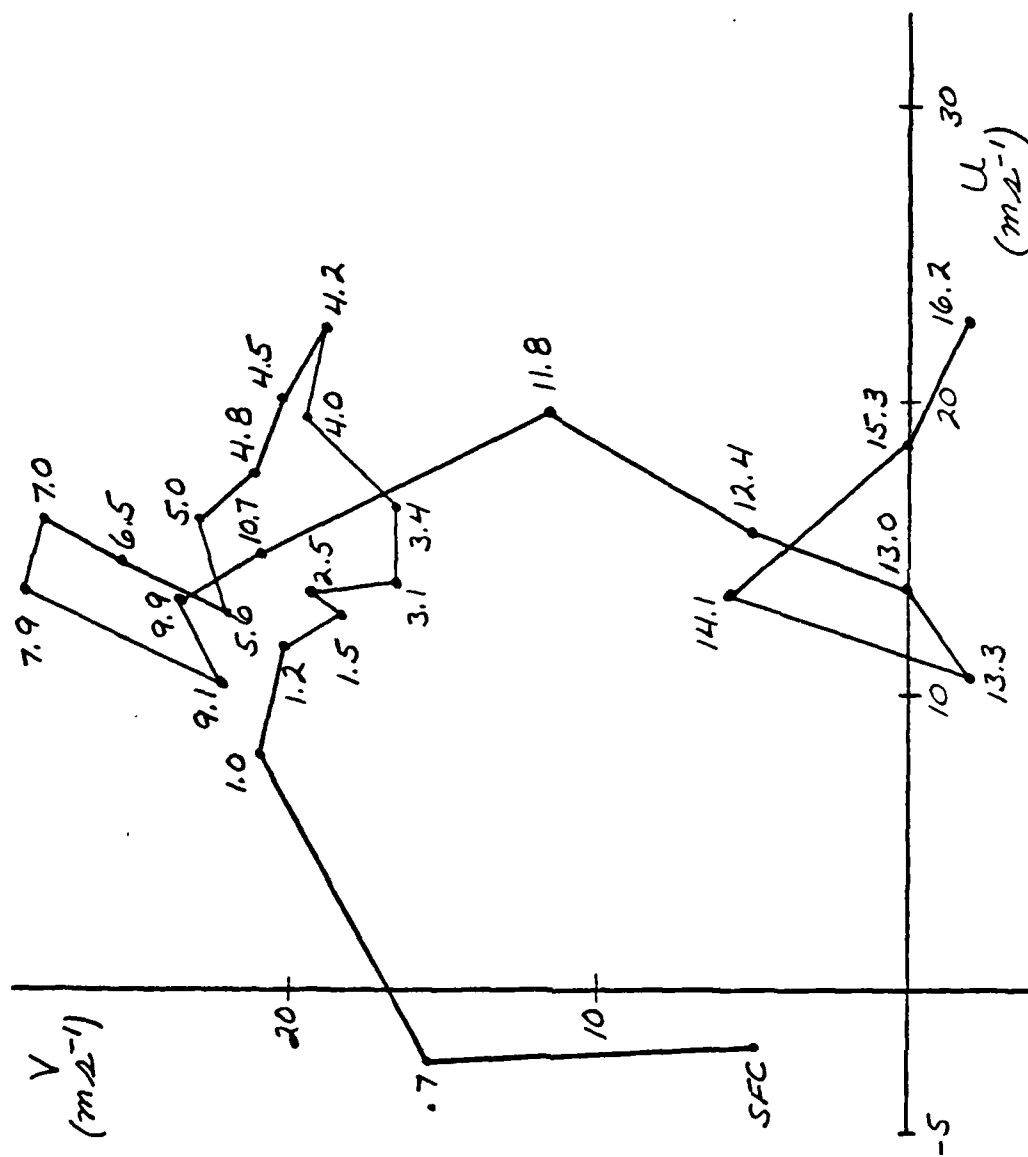


Fig. 29. Hodograph of winds from Oklahoma City sounding 0600 CST, 5 December 1975. Surface wind from near time and location of bell-shaped storm formation. Heights in km.

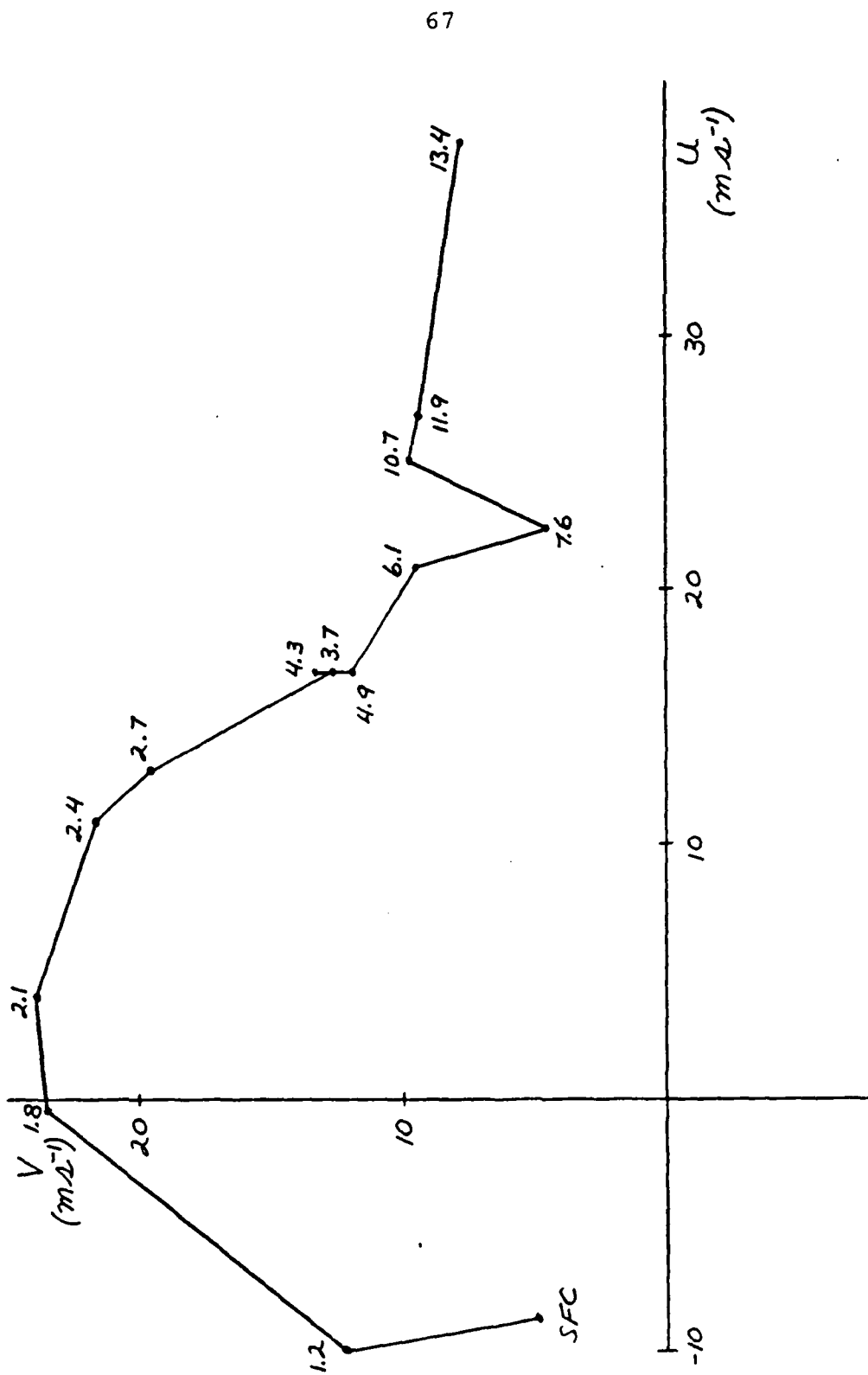


Fig. 30. Composite hodograph of winds from 0600 and 1800 CST, 26 April 1976 soundings at Amarillo. Surface wind from near time and location of bell-shaped storm formation. Heights in km.

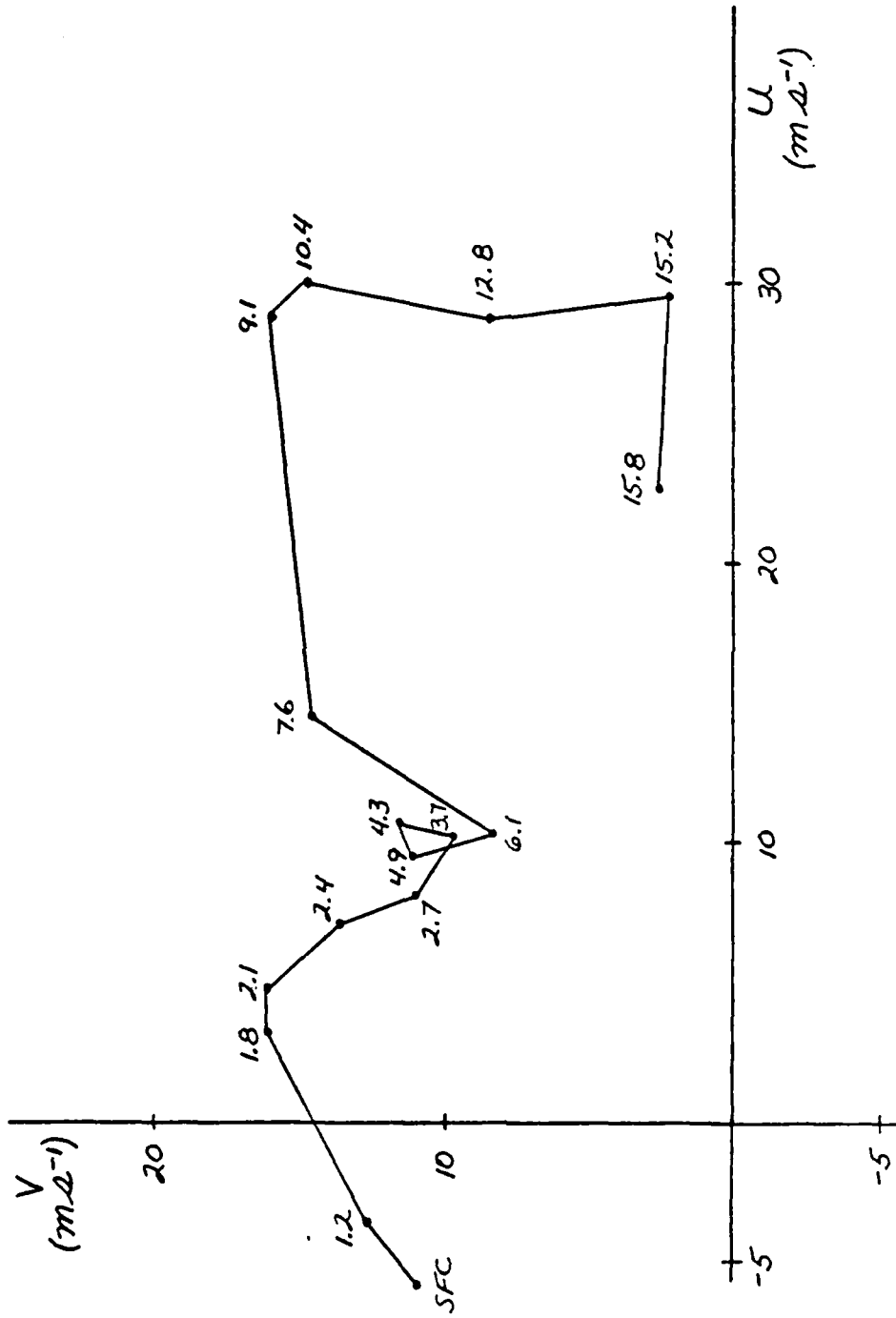


Fig. 31. Composite hodograph of winds from 0600 and 1800 CST, 27 April 1976 soundings at Amarillo. Surface wind from near time and location of bell-shaped storm formation. Heights in km.

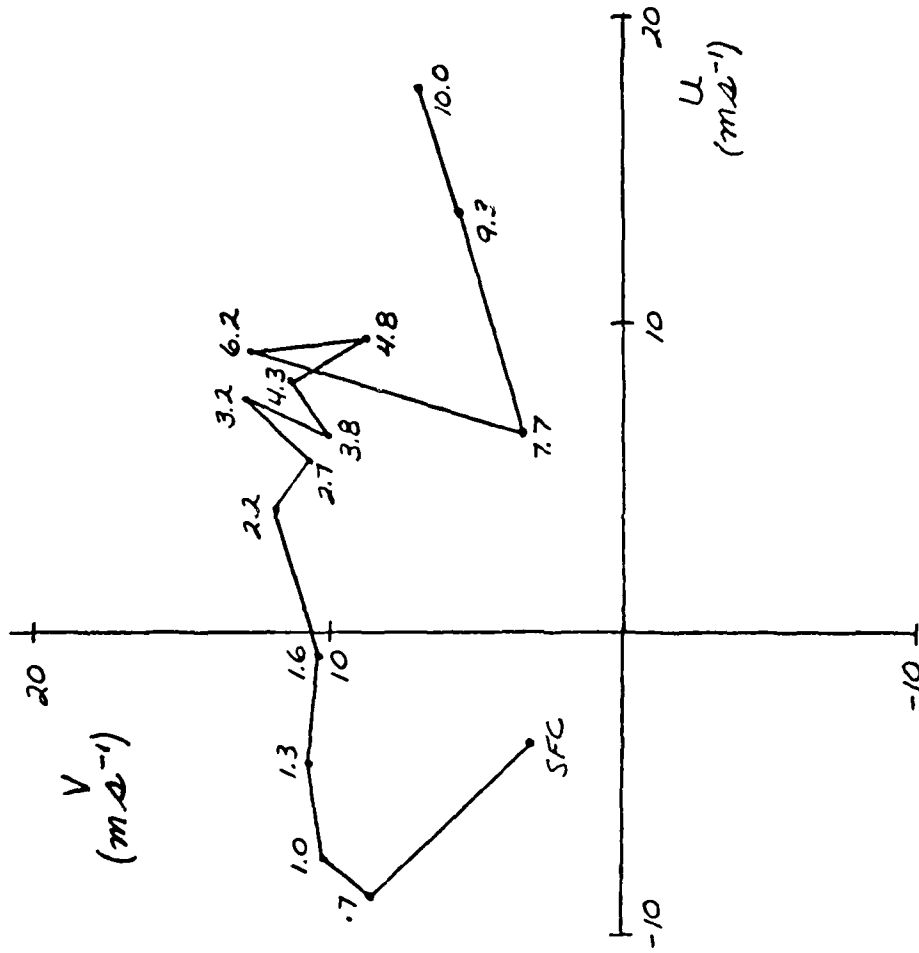


Fig. 32. Composite hodograph of winds from 0600 and 1800 CST, 30 April 1978 soundings at Oklahoma City. Surface wind from near time and location of bell-shaped storm formation. Heights in km.

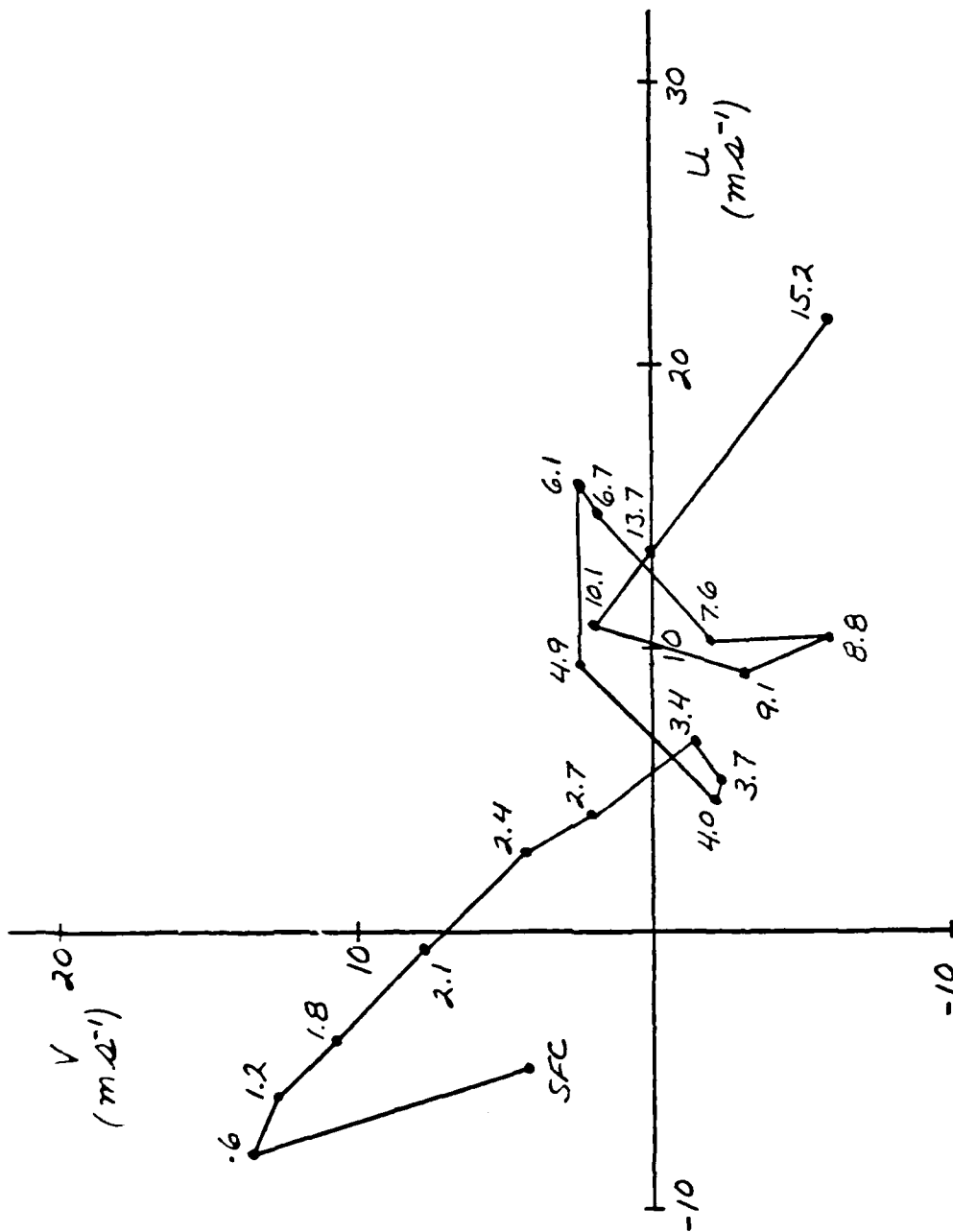


Fig. 33. Hodograph of winds from Stephenville, TX sounding 1800 CST, 16 May 1978. Surface wind from near time and location of bell-shaped storm formation. Heights in km.

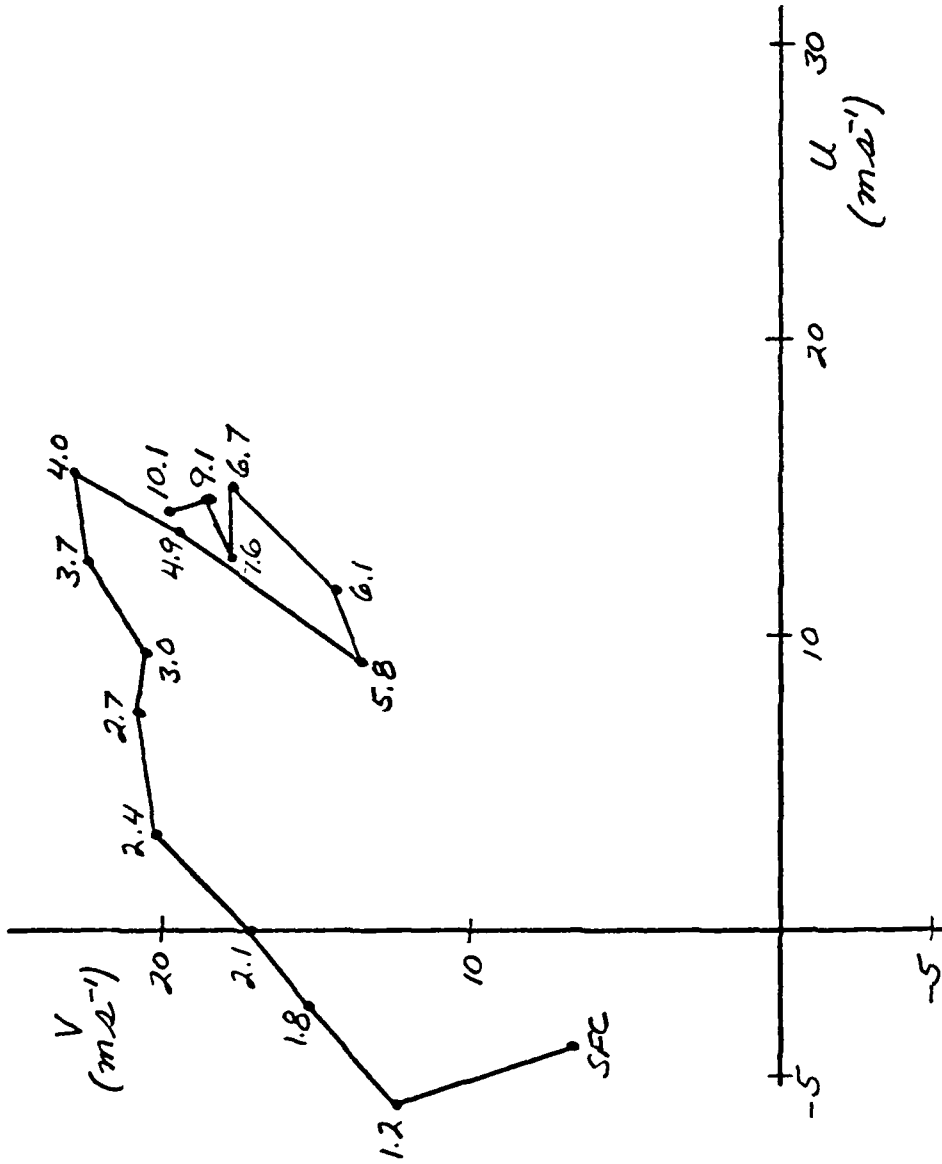


Fig. 34. Hodograph of winds from Amarillo sounding 1800 CST, 24 May 1978. Surface wind from near time and location of bell-shaped storm formation. Heights in km.

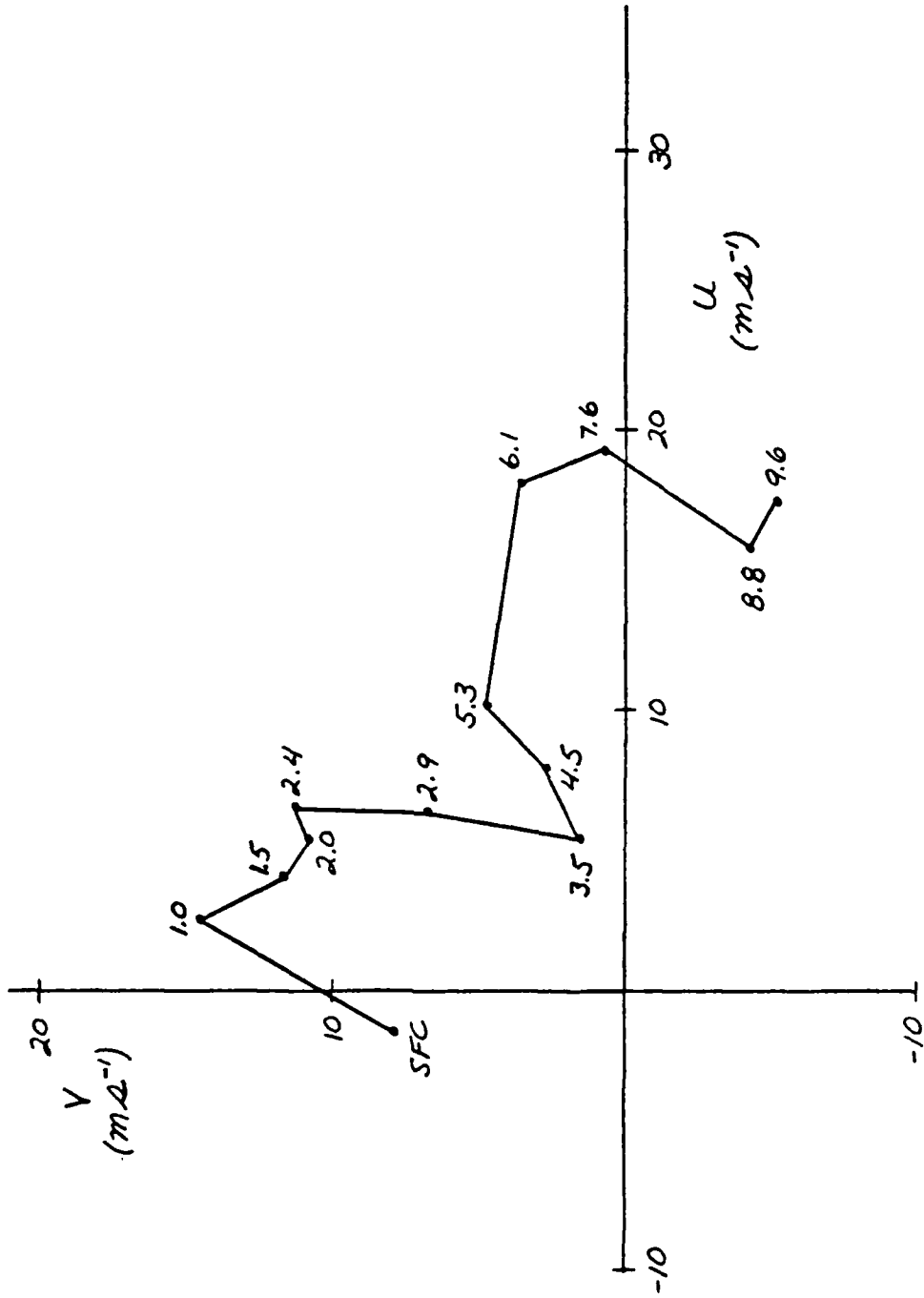


Fig. 35. Composite hodograph of winds from 0600 and 1800 CST, 30 May 1978 soundings at Dodge City. Surface wind from near time and location of bell-shaped storm formation. Heights in km.

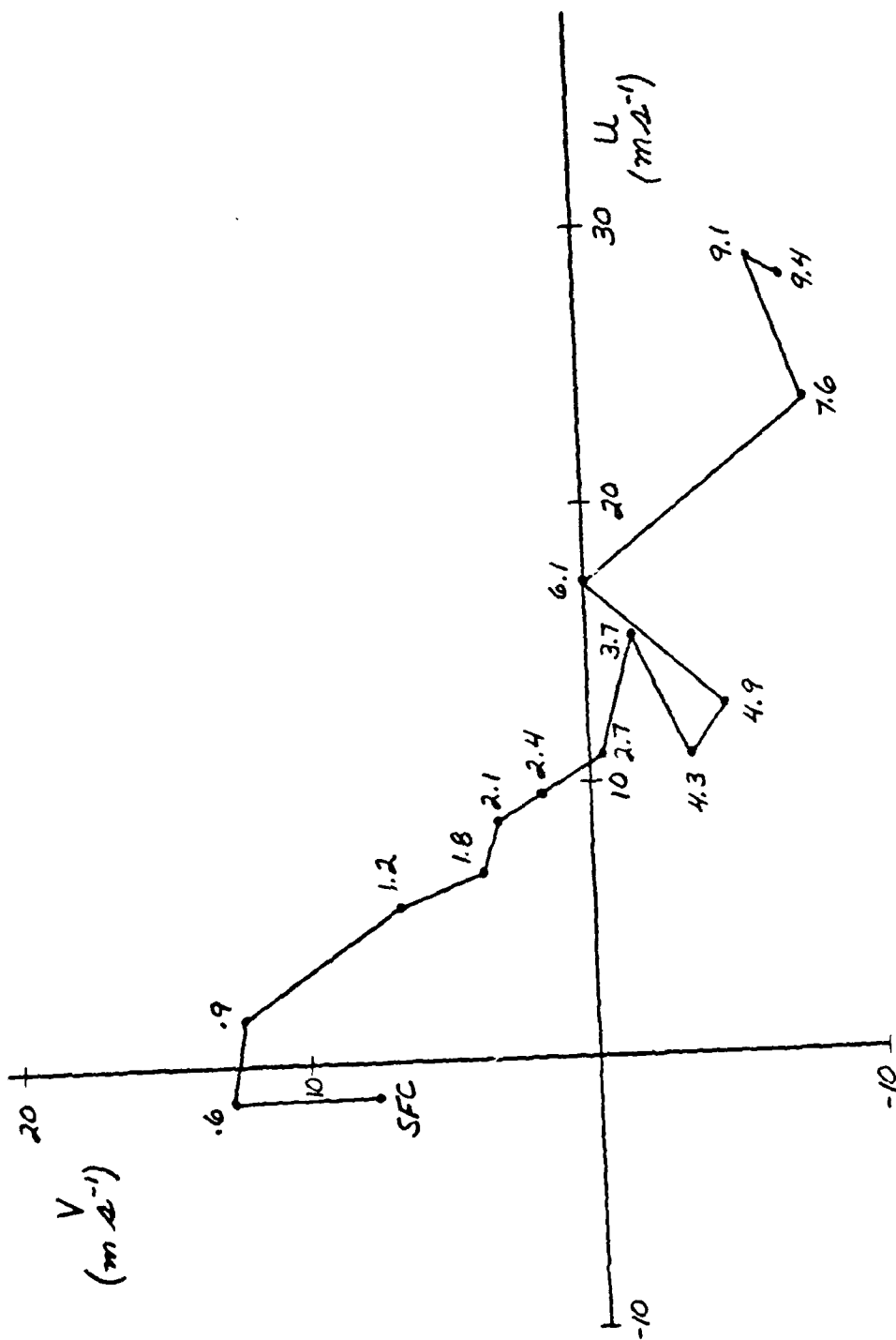


Fig. 36. Composite hodograph of winds from 0600 and 1800 CST, 20 June 1979 soundings at Oklahoma City. Surface wind from near time and location of bell-shaped storm formation. Heights in km.

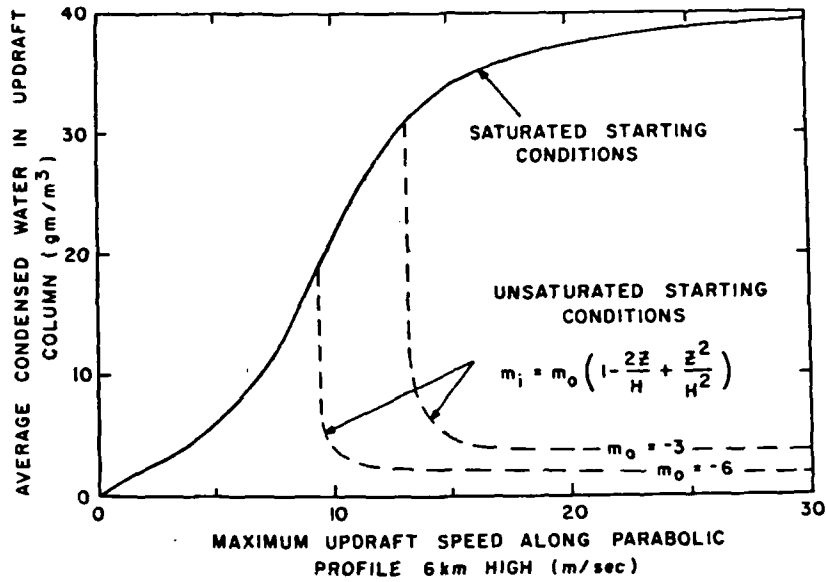


FIG. 14.20. Average steady-state condensed water content in relation to maximum updraft speed and initial moisture profile in a compressible atmosphere.

Fig. 37. Water Content in relation to updraft speeds. (From Kessler, 1969). The initial sub-saturation is given by m_o .

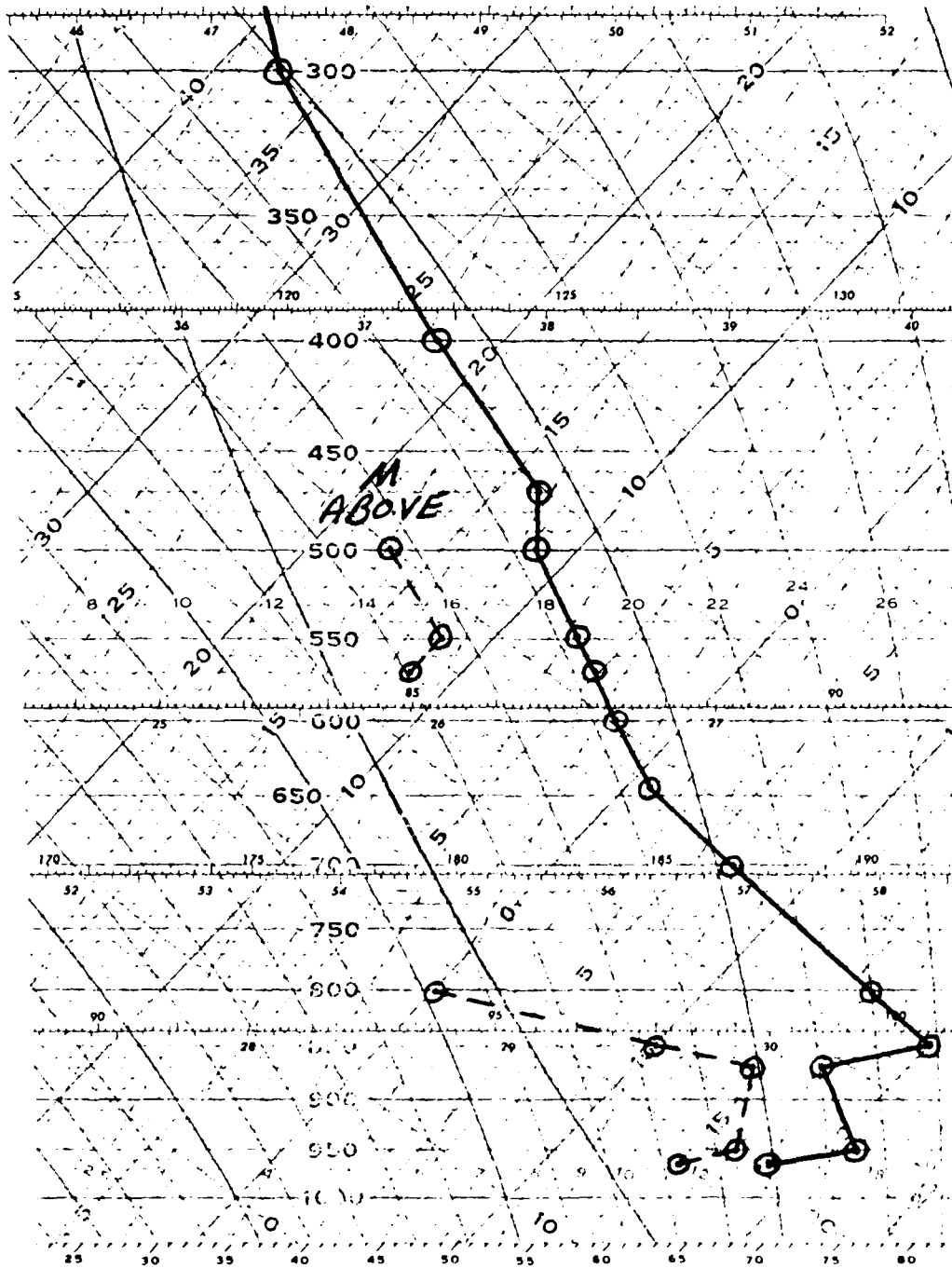


Fig. 38. Model morning sounding for days of bell-shaped storm occurrence.

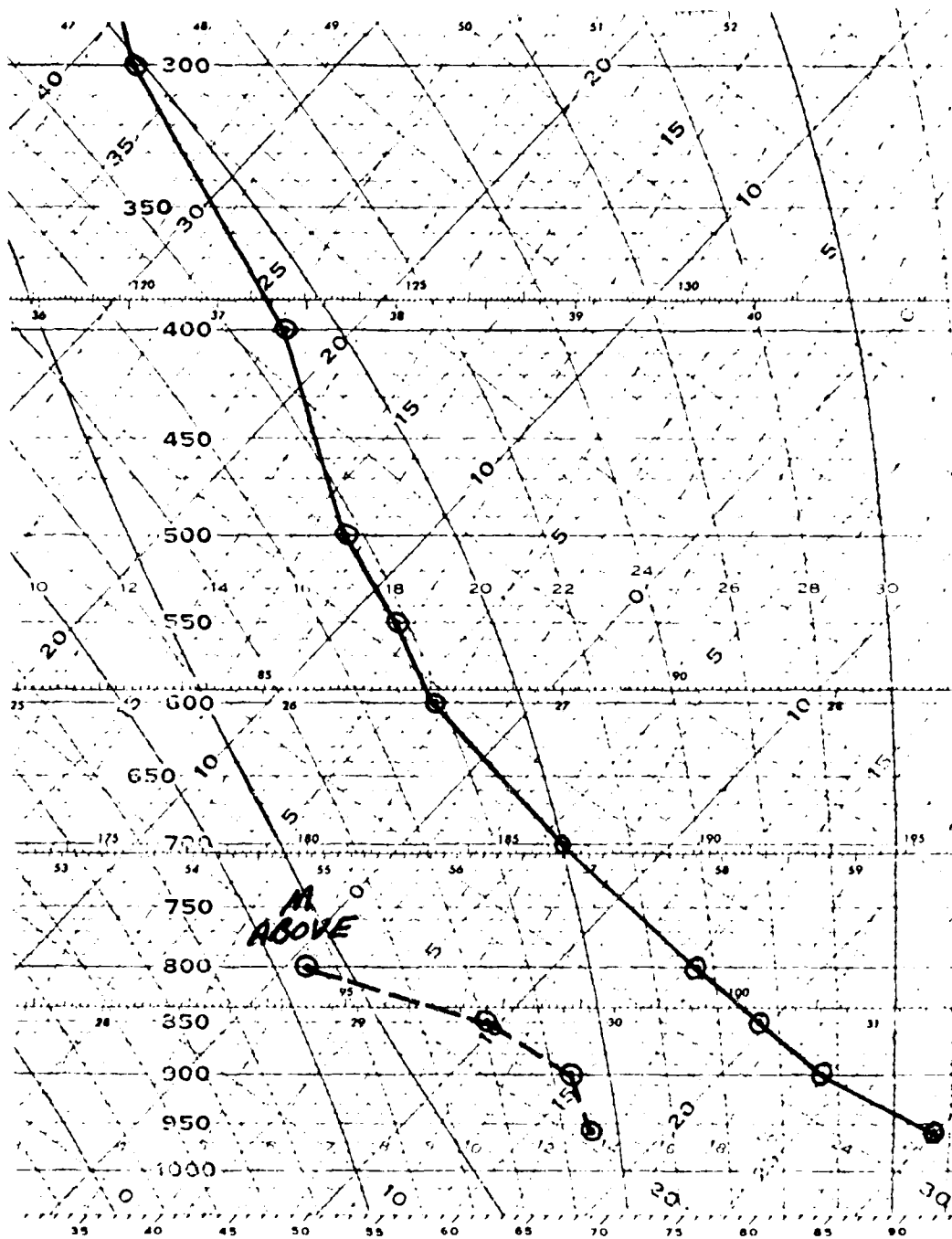


Fig. 39. Model sounding near time of bell-shaped storm development.

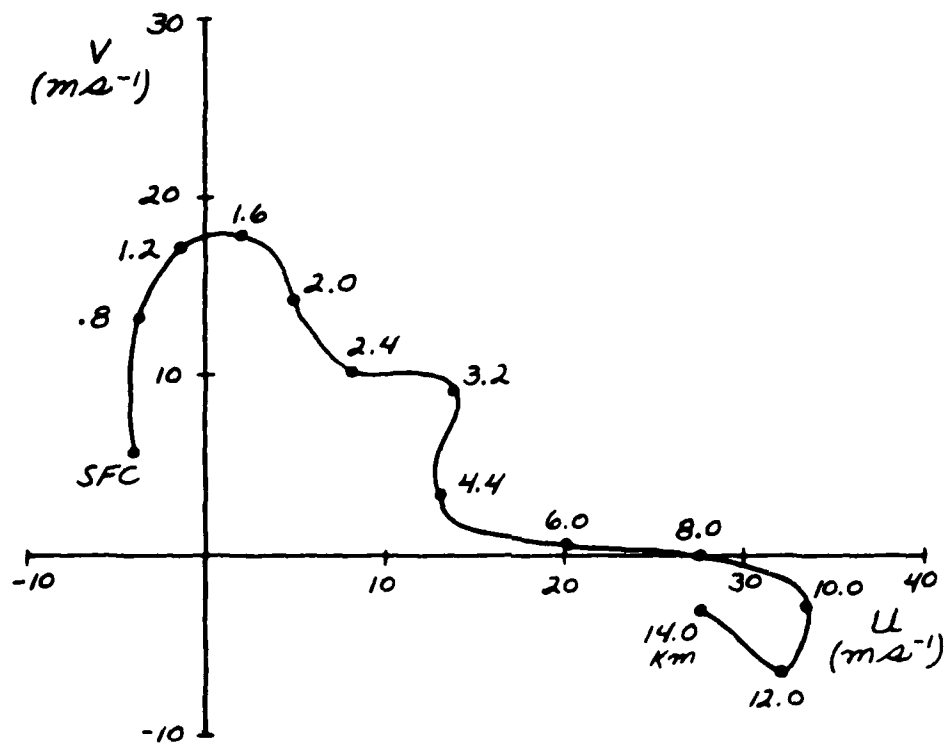


Fig. 40. Model hodograph of environmental winds near bell-shaped storms.

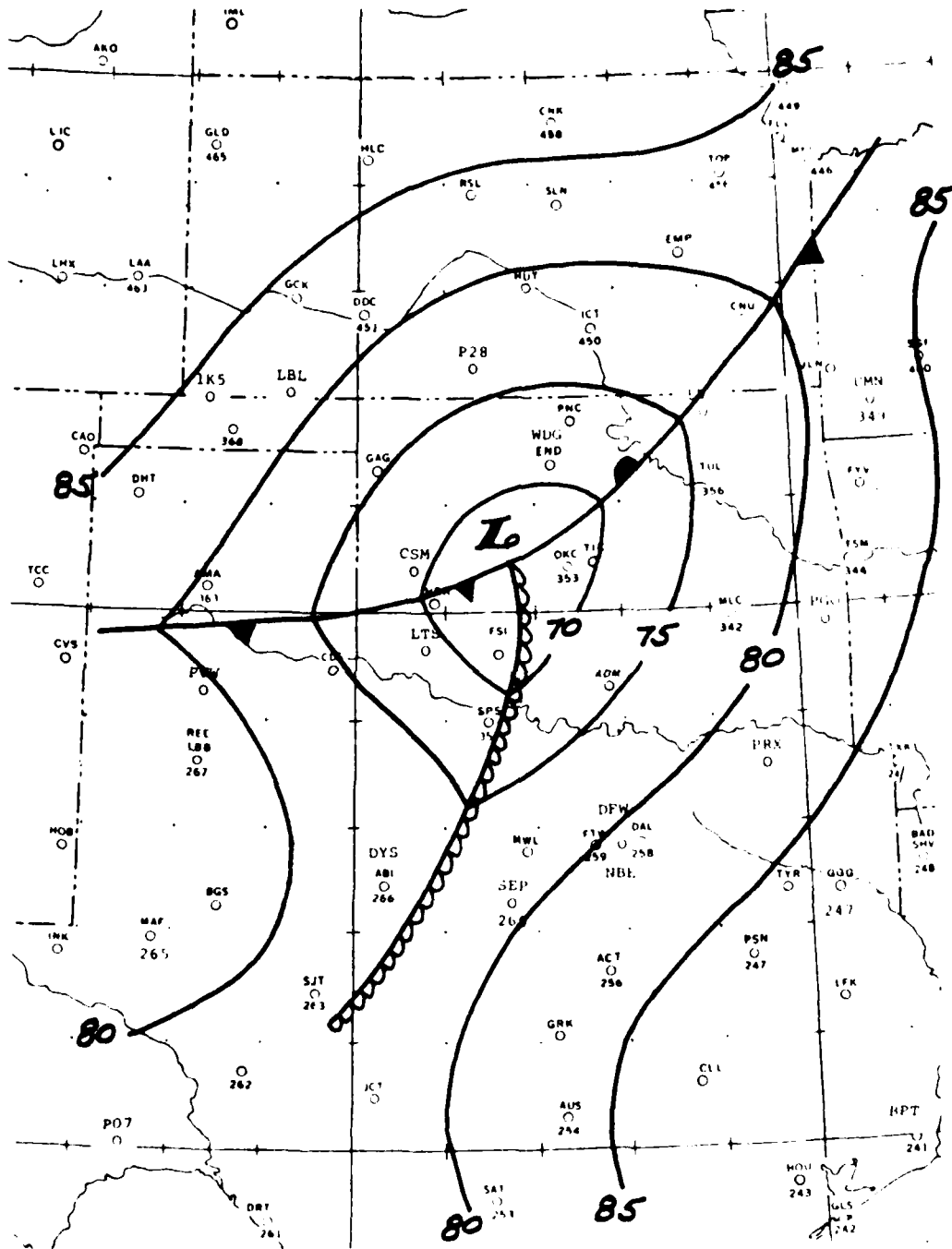


FIG. 41. Model surface features near time of bell-shaped storm development.

Table 1. Thermodynamic parameters of the environment in which bell-shaped storms occur

Case	Thermal buoyancy at 500 mb using parcel method (°C)	Depth of Moist Layer (AGL) (m)	Moist Layer Mixing Ratio (gm kg ⁻¹)	Convective Condensation Level (MSL) (km)
26 May 63	+ 8.4	700	14.0	2.1
4 June 73	+10.4	975	15.3	2.1
5 June 74	+ 8.0	1300	10.8	3.3
5 Dec. 75	+ 5.7	2050	11.0	1.1
26 Apr. 76	+ 5.2	735	8.2	3.2
27 Apr. 76	+ 9.3	1320	10.6	2.8
30 Apr. 78	+10.1	1420	12.8	1.9
16 May 78	+ 8.0	1100	13.0	2.4
24 May 78	+ 6.6	1300	11.0	3.0
30 May 78	+ 7.7	1310	9.8	3.0
20 June 79	+ 6.1	1540	13.4	2.3
Average	+ 7.8	1250	11.8	2.5

Table 2. Stability and wind shear parameters of the environment in which bell-shaped storms occur

CASE STUDY	Thermal buoyancy at 500 mb using parcel method ($^{\circ}\text{C}$)	Veering in subcloud layer (deg)	Mean wind in subcloud layer ($\text{deg}/\text{m s}^{-1}$)	Mean wind surface to 10 km ($\text{deg}/\text{m s}^{-1}$)	Storm Motion ($\text{deg}/\text{m s}^{-1}$)	Shear in cloud layer (10^{-3} s^{-1})
26 May 1963	+ 8.4	80	190/13	255/25	270/10	4.0
4 June 1973	+10.4	55	205/15	235/18	250/11	3.8
5 June 1974	+ 8.0	105	205/13	240/14	270/8	3.9
5 Dec. 1975	+ 5.7	45	195/17	210/25	225/10	3.5
26 April 1976	+ 5.2	100	180/21	220/21	270/5	2.8
27 April 1976	+ 9.3	65	190/15	215/19	240/10	3.4
30 April 1978	+10.1	60	160/11	210/13	230/8	3.1
16 May 1978	+ 8.0	80	170/10	240/10	-----	2.9
24 May 1978	+ 6.6	55	180/17	200/20	230/12	3.2
30 May 1978	+ 7.7	60	205/12	240/14	280/8	3.5
20 June 1979	+ 6.1	90	215/10	255/16	-----	3.6
Average	+ 7.8	72.3	190/14.0	229/17.3	252/9.1	3.4

Table 3. Thermodynamic Stability and Wind Shear Parameters for Certain Well-Documented Supercell Storms
(after Marwitz, 1972a and Brown, 1976)

CASE STUDY	Thermal buoyancy at 500 mb using parcel method ($^{\circ}\text{C}$)	Veering in subcloud layer (deg)	Mean wind in subcloud layer ($\text{deg}/\text{m s}^{-1}$)	Mean wind surface to 10 km ($\text{deg}/\text{m s}^{-1}$)	Storm motion ($\text{deg}/\text{m s}^{-1}$)	Shear in cloud layer (10^{-3}s^{-1})
Browning & Donaldson (1963)	+4	50	180/17	260/27	255/10	2.5
Browning (1965)	+8	80	190/13	255/25	270/10	4.0
Haglund (1969)	+5	60	206/13	265/25	280/14	2.5
Marwitz & Berry (1970)	+9	90	190/10	250/17	285/14	4.5
Marwitz (1972)	+5	60	160/11	250/15	320/9	4.0
Brown (1976)	+8	60	227/9	268/19	283/10	3.7
Ray (et al., (1975)	+6	60	190/20	220/34	220/15	3.7
Heymsfield (1978)	+5	40	190/18	240/25	255/12	3.0
Nelson (1980)	+8	60	190/7	260/15	270/13	2.6
Average	+6.4	62	191/13.1	252/22.4	271/11.9	3.4

Table 4. Thermodynamic Stability and Wind Shear Parameters for Certain Well-Documented Multi-cell Storms
(after Marwitz, 1972b)

CASE STUDY	Thermal buoyancy at 500 mb using parcel method (°C)	Veering in subcloud layer (deg)	Mean wind in subcloud layer (deg/m s ⁻¹)	Mean wind surface to 10 km (deg/m s ⁻¹)	Storm Motion (deg/m s ⁻¹)	Shear in cloud layer (10 ⁻³ s ⁻¹)
Browning & Ludlam (1960)	+1	160	150/8	210/21	255/18	2.5
Christholm (1966) 18 Jul 64	+4	40	240/7	235/26	250/12	---
Christholm (1966) 21 Jul 64	+4	-90	250/6	230/17	250/10	---
Alhambra 12 Jul 69	+2	30	020/30	245/11	300/9	2.0
Rimbey 16 Jul 69	+4	30	150/4	240/11	240/11	2.0
Benalto 17 Jul 68	+3	45	150/4	265/7	305/9	1.5
Sylvan Lake 25 Jul 68	+6	80	010/4	275/13	315/16	2.0
Carstairs 17 Jul 69	+4	120	250/3	265/15	295/12	4.0
Butte 11 Jul 70	+7	10	140/6	235/16	310/8	4.5
Average	+3.9	47.2	151/8.0	244/15.2	280/11.6	2.6

Table 5. Hodograph turning with height for bell shaped storms

Case	θ (deg)	H (km)	$\frac{\theta \text{ (deg)}}{H \text{ (km)}}$
26 May 1963	60	1.5	40.0
4 June 1973	50	1.8	27.8
5 June 1974	35	1.8	19.4
5 Dec. 1975	45	1.5	30.0
26 April 1976	115	3.7	31.1
27 April 1976	70	2.7	25.9
30 April 1978	40	1.6	25.0
16 May 1978	25	1.8	13.9
24 May 1978	30	2.1	14.3
30 May 1978	30	1.5	20.0
20 June 1979	70	1.8	38.9
Average	51.8	2.0	26.0

Table 6. Hodograph turning with height for certain well documented supercell storms

Case	θ (deg)	H (km)	$\frac{\theta \text{ (deg)}}{H \text{ (km)}}$
Ray <i>et al.</i> (1975)	62	2	31.0
Heymsfield (1978)	42	2	21.0
Marwitz (1972a)	130	5	26.0
Browning & Donaldson (1963)	50	1.9	26.3
Brown (1976)	90	2	45.0
Nelson (1980)	115	3.5	32.9
Average	81.5	3.4	23.7

AD-A106 158

AIR FORCE INST OF TECH WRIGHT-PATTERSON AFB OH
SYNOPTIC CLIMATOLOGY OF BELL-SHAPED THUNDERSTORMS. (U)
1981 C R PARKS
AFIT-CI-81-27T

F/G 4/2

UNCLASSIFIED

NL

2 OF 2
CO A
SERIAL



END
DATE
FILMED
11-81
DTIC

Table 7. Key parameters in forecasting severe storms.

RANK	PARAMETER	WEAK	MODERATE	STRONG
1	500 mb Vorticity	Neutral or Negative Vort Advection	Contours Cross Vort Pattern 30°	Contours cross at more than 30°
2	Stability	Lifted Index	-2	-3 to -5
	Totals	50	50 to 55	55
3	Middle Level	Jet Shear	35K 15K/90 nm	35K-50K 15K-30K 90 nm
	Upper Level	Jet Shear	55K 15K 90 nm	55 to 85K 15K - 30K 90 nm
4	Low-Level Jet	20K	25K - 34K	35K
5	Low-Level Moisture	8	8 to 12	12
6	850-mb Max-Temp Field	E of Moist Ridge	Over Moist Ridge	W of Moist Ridge
7	700-mb No-Change Line	Winds Cross Line 20°	Winds Cross Line 20° to 40°	Winds Cross Line 40°
8	700-mb Dry-Air Intrusion	Not Available - or Available but weak Wind Field	Winds from Dry to Moist Intrude at an Angle of 10 to 40° are at least 15K	Winds Intrude at an Angle of 40° and are at least 25K
9	12-hr Sfc Pressure Falls		1 to 5 MB	5MB
10	500-mb Height Change	30 m	30 to 60 m	60 m
11	Height of Wet-Bulb-Zero above Sfc	Above 11000 ft Below 5000 ft	9000 to 11000 ft 5000 to 7000 ft	7000 to 9000 ft
12	Surface Pressure over Threat Area	1010 mb	1010 to 1005 mb	1005 mb
13	Sfc Dew Point	55° F	55° to 64° F	65° F